Cancer Nanotechnology

RESEARCH Open Access

Artemisinin-loaded polylactic acid nanoparticles alleviate 1.2 *N,N*-dimethylhydrazine-induced colorectal cancer in Albino rats

Zeinab Dwidar[1*], Walaa F. Awadin[1], Mohamed El-Adl[2], Mohamed Abomosallam[3], Aya Aly ELzeer[4] and Ahmed M. Abdellatif[5]

*Correspondence:
dzeinab17@gmail.com

[1] Department of Pathology, Faculty of Veterinary Medicine, Mansoura University, Mansoura 35516, Egypt
[2] Department of Biochemistry and Molecular Biology, Faculty of Veterinary Medicine, Mansoura University, Mansoura 35516, Egypt
[3] Department of Forensic Medicine and Toxicology, Faculty of Veterinary Medicine, Mansoura University, Mansoura 35516, Egypt
[4] Department of Development of Animal Wealth, Faculty of Veterinary Medicine, Mansoura University, Mansoura 35516, Egypt
[5] Department of Anatomy and Embryology, Faculty of Veterinary Medicine, Mansoura University, Mansoura 35516, Egypt

Abstract

Background: Colorectal cancer (CRC) is one of the most fatal malignant neoplasms around the world. Artemisinin (ART) displays broad anticancer properties with some drawbacks. Therefore, we tried to enhance the anticancer efficacy of ART by loading it into polylactic acid nanoparticles (ART-PLA NPs) and investigated its ameliorative effect against 1.2 *N,N*-dimethylhydrazine (DMH) induced CRC through targeting wnt/β-catenin and NF-κB pathways.

Methods: Sixty male rats were allocated into six groups: control, ART, ART-PLA NPs, DMH, DMH + ART and DMH + ART-PLA NPs. Rats were administered 7 mg/kg /bw of ART and ART-PLA NPs daily for 24 weeks and 40 mg/kg bw, i.p of DMH once a week for successive 12 weeks.

Results: ART and ART-PLA NPs significantly decreased carcinoembryonic antigen (CEA) serum concentration, inhibit NF-κB pathways through mitigation of the proinflammatory cytokines TNF-α, IL-1β, and NF-kB-p65, and enhanced the anti-inflammatory cytokine IL-10 colonic levels. The histopathological study of DMH group revealed moderate to severe dysplasia, different types of adenoma and adenocarcinoma with reduced colonic mucous secretion and increased fibrous tissue deposition. ART-PLA NPs treatment was more powerful than ART as indicated by fewer and smaller colorectal tumors, higher mucous secretion and mild fibrous tissue deposition. DMH treatment upregulated *β-catenin* gene expression in the colonic mucosa. Surprisingly, *β-catenin* mRNA level appeared significantly lower in DMH + ART and DMH + ART-PLA NPs groups than DMH group, with a more pronounced decline in the ART-PLA NPs group. While, *adenomatous polyposis coli* (*APC*) gene expression was significantly downregulated in DMH group than other groups, and its expression appeared potentiated by DMH + ART and DMH + ART-PLA NPs treatments. Moreover, the gene expression findings were confirmed by western blot analysis of β-catenin and APC protein expression that recorded the same expression pattern.

Conclusion: This study suggests ART-PLA NPs attenuated cancer cell proliferation via targeting wnt/β-catenin and NF-κB pathways than free ART. Thus it should be considered when formulating prophylactic and therapeutic strategies for CRC.

Keywords: Colorectal cancer, 1,2 *N*,*N* dimethylhydrazine, ART, ART-PLA NPs

Introduction

Colorectal cancer (CRC) is ranked as the third most common malignant neoplasm and the second leading cause of death around the world, accounting for 600,000 deaths annually (Sharma et al. 2017; Dekker et al. 2019). By 2030, it is predicted that the worldwide morbidity rate will rise to 1.1 million (Sung et al. 2021). The spread and advancement of CRC are thought to be significantly influenced by a number of predisposing variables, including dietary and lifestyle habits, family history, chronic inflammation, microbial exposure and changed gut microbiota (Cunningham 2010; Brenner and Chen 2018; Dekker et al. 2019). A variety of genetic and epigenetic alterations occur during the process of colon carcinogenesis giving the tumor cells the ability to proliferate their progeny (Nguyen et al. 2020). The colon carcinogenesis is a multistep process that can be progressed from dysplastic lesions, adenomas, to adenocarcinomas (Idikio 2011). Colon epithelial cell dysplasia represents the early preneoplastic histological alterations of colon cancer which may be low or high grade dysplasia. Also defined as any changes in the structure and cytology of the epithelium that make an organ more vulnerable to the development of cancer (Boivin et al. 2003). Adenomas are restricted to the mucosal layer and can be classified as mild, moderate, or severe depending on the degree of dysplasia, the complexity degree of glandular or villous structures, the nuclear morphology and the extent of stratification (Cerar et al. 2004). While malignant lesions, known as adenocarcinomas can invade the submucosa after passing through the muscularis mucosa (Hong 2014). There are many subtypes of CRC according to WHO histological classification (Nagtegaal et al. 2019). CRC may be medullary, mucinous, signet ring cell, adenosquamous, cribriform comedo-type, micropapillary, serrated or spindle cell type (Fleming et al. 2012). CRC results from mutations affecting the tumor suppressor genes, oncogenes, and genes responsible for DNA repair mechanisms (Mármol et al. 2017; Nojadeh et al. 2018). Leading to change in about 500 gene products that affect various cell functions and control several signalling pathways. These products include transcription factors, growth factors and their receptors, proapoptotic and proapoptotic proteins, inflammatory cytokines and enzymes beside tumor suppressors (Aggarwal et al. 2013). Moreover, there are many signalling pathways dysregulated during colon carcinogenesis such as Wnt/β-catenin and nuclear factor kappa B (NF-κB) and other implicate in proliferation, survival and self-renewal features of the malignant cells (Silva et al. 2021). As a result CRC could be further classified into three different types according to the mutation origin to Sporadic 70%, familial 25% and inherited CRC 5% of recorded CRC cases (Alzahrani et al. 2021).

Due to the similarity between the pathogenesis of colorectal cancer in rats and humans, 1,2-dimethylhydrazine (DMH), a powerful carcinogen, is frequently employed to induce colorectal cancer (Perše and Cerar 2005). DMH and its derivative, azoxymethane (AOM), convert to their final reactive product called methylazoxymethanol (MAM). MAM is metabolized in the liver and gives methyldiazonium ions that induce macromolecules alkylation. Then, they reach the colon by bile, where they

cause oxidative stress and further DNA alkylation leading to gene mutation and carcinogenic metabolites (Keshavarz et al. 2011; Sadik 2013).

Artemisinin is an extract of a Chinese herb called Artemisia annua, also called Qinghao or Sweet worm wood (Badshah et al. 2018; Talman et al. 2019). ART and its derivatives including dihydroartemisinin, arteether, artemether and artesunate were widely used as anti-malarial drugs (Ashley and White 2005). In addition to their anti-malarial activities, they have anti-parasitic (Lam et al. 2018), antimicrobial (Appalasamy et al. 2014), antiviral (Roy et al. 2015) and anticancer activities (Aderibigbe 2017; Efferth 2017; Zhang et al. 2018). ART still has some drawbacks, including poor solubility in water and oil, low bioavailability, initial burst effect in vivo that identified by high peak plasma concentrations and accelerated metabolism (Chen et al. 2009; Zeng et al. 2023). Therefore, development of carriers that could improve ART pharmacokinetic properties is essential for effective therapy (Allen and Cullis 2004). Currently, nanosize drug delivery devices are significant components of modern medicine with a wide range of therapeutic uses due to their capacity to modify pharmacokinetics and biodistribution of the drugs (Bilia et al. 2017). Polylactic acid (PLA) is a potent biodegradable polymer used for nanoparticles development. PLAnanoparticles interact with host cells in a way that is appropriate and are not harmful to human biology. In addition, PLA nanoparticles took the approval of Food and Drug Administration (FDA) as it did not revealed any cytotoxic effect on different cell lines (Feng et al. 2019). Moreover, it has promising tensile strength and good release capacity providing suitable time span before the degradation reactions (Casalini et al. 2019). It has extended surface area, high drug loading capacity, ligand functionalization feasibility, stable storage, and flexibility in management strategies (Feng 2004; Fattahi et al. 2019; Xu et al. 2020; Buabeid et al. 2020). PLA nanoparticles was used as a nanocarrier for enhancement of many herbal drugs as catechin and curcumin or anti-cancer remedy as oxorubicin, docetaxel, paclitaxel, irinotecan and 5-fluorouracil. It provided suitable encapsulation efficiency and good loading capacity in various studies operated on many cancer cell lines and animal models for treatment of CRC, breast cancer, liver cancer, leukemia, glioma, prostate, pancreatic, osteosarcoma and ovarian cancer (Fattahi and Zamani 2022). Interestingly, PLAnanoparticles can undergo passive targeting of the malignant tissue and provides sustainable release leads to improving tumor-specific delivery efficacy. It can enter the cells by endocytosis and escape from the leaky, defective blood vessels and defective lymphatic drainage by "enhanced permeation and retention" mechanism so they could accumulate in the solid tumors (Brannon-Peppas and Blanchette 2004; Yallapu et al. 2010; Maeda et al. 2013). Thus, PLAnanoparticles are considered good applicable carriers for delivery of the anti-cancer drugs (Mishra et al. 2010). As a result, this study aims to investigate anticancer efficacy of ART by loading it into polylactic acid nanoparticles and its ameliorative effect against 1.2 *N*,*N*-dimethylhydrazine (DMH)-induced colorectal cancer through targeting wnt/β-catenin and NF-κB pathways.

Materials and methods

Animals

Sixty six-week-old adult male albino rats weighing 130–140 g were obtained from the Medical Experimental Research Center (MERC) animal house in Faculty of Medicine, Mansoura University. The rats were accommodated for 1 week before the start of the

experiment in the Faculty of Veterinary Medicine animal room, Mansoura University, Egypt. The temperature and relative humidity conditions were adjusted to 22 ± 2 °C and 50 ± 5%, respectively, with a 12-h light–dark cycle. A clean, balanced pellet diet was provided with fresh tap water ad libitum.

Chemicals

1.2 *N*,*N*-dimethylhydrazine (DMH) was obtained from Sigma–Aldrich Chemical Company (Spruce St. Saint Louis, MO, United States, D161802). Artemisinin extract powder, purity (approximately 99%), purchased from Xi'an Longze Biotechnology Co., LTD, China. polylactic acid purchased from NatureWorks LLC (Mw; 199,590 Da, NatureWorks® IngeoTM 2002D), acetone, dichloromethane (DCM) and polyvinyl alcohol (PLA) (Mw; 1,15,000 Da) obtained from Loba Chemie, Mumbai, India. Rat Enzyme-Linked Immunosorbent Assay (ELISA) Kit for Tumor Necrosis Factor-α (TNF-*α*) (Cat. No. E0764Ra), Interleukin 1 beta (IL-1β) (Cat. No. E0119Ra) and Interleukin 10 (IL-10) (Cat. No. E0108Ra) were purchased from Bioassay technology laboratory (Shanghai Korain Biotech Co Ltd). Nuclear factor kappa B (NF-kB-p65) (Cat. No. E-EL-R0674) and Carcinoembryonic Antigen (CEA) (Cat. No. E-EL-R0150) were purchased from Elabscience® (USA). cDNA synthesis kit (SensiFAST™ cDNA Synthesis Kit, Catalog number: BIO-65053) and SYBR Green Master Mix (2 × SensiFast™ SYBR) were purchased from Bioline (USA). For western blot analysis, we purchased APC (F-3): SC-9998 (Santa Cruz Biotechnology, Inc.) antibody and β-Catenin Antibody (#9562) (Cell Signaling Technology, USA).

Preparation of ART-loaded PLA NPs

PLA nanoparticles were prepared through the single-emulsion solvent evaporation technique with slight modifications (Reis et al. 2006). In brief, an aqueous solution of PVA (1%, w/v) was prepared by heating the required concentration at 90 °C until it was completely dissolved and then cooled at room temperature. Afterwards, 150 mg of PLA was dissolved in organic solvents (4 mL DCM and 1 mL acetone) then 50 mg ART was added to the same volume. This mixture was carefully added to 30 mL of the previously prepared PVA solution and emulsified using a probe sonicator at 20 kHz for 5 min (Q500, Qsonica, Newtown, USA). Next, the organic solvent was evaporated with a rotatory evaporator at 37 °C for 40 min (Büchi R-205, Essen, Germany). Then the mixture subjected to centrifugation at (10,000 rpm for 30 min), washed twice for removal of the surfactant and stored at 4 °C for further analysis.

Characterization of ART-loaded PLA NPs

ART-PLA NPs size and morphology were evaluated by a transmission electron microscope (TEM, JEOL-2000 EX-II, Tokyo, Japan) at 200 kV. For proper determination of shape and size, the samples were assessed in triplicate; a drop of the sample was positioned into a carbon-coated grid and then dried under vacuum before capturing the TEM images.

Encapsulation efficiency (EE) of ART-PLA NPs

The encapsulation efficiency (EE) of ART-PLA NPs was measured with UV-spectrophotometer at 420 nm after generating a calibration curve. Then it is calculated by the following equation

$$\mathrm{EE}(\%) = \frac{\text{Total amount of the drug} - \text{Freeamount of the drug}}{\text{Total amount of the drug}} \times 100$$

Colorectal cancer induction

1.2 *N*,*N*-dimethylhydrazine was freshly prepared in 1 mM/L EDTA before administration and the pH was adjusted to 7.0 by NaOH diluted solution. Rats were subjected to intraperitoneal injection of DMH (40 mg/kg/bw) once a week for 12 successive weeks (de Paula Carli et al. 2012; Jia et al. 2014; Zhu et al. 2014).

Experimental design

Sixty weight-matched, healthy, acclimatized male albino rats were divided into six groups ($n = 10$). Group (1): Control group maintained on rat pellet ration and clean tap water without medication. Group (2): ART group received ART (7 mg/kg/bw) daily for 24 weeks by oral gavage (Lai and Singh 2006; Boareto et al. 2008; Farombi et al. 2014; Patyar et al. 2017). Group (3): ART-PLA NPs group received ART-PLA NPs (7 mg/kg/bw) daily for 24 weeks by oral gavage (Boareto et al. 2008; Lai and Singh 2006; Farombi et al. 2014; Patyar et al. 2017). Group (4): DMH group exposed to intraperitoneal injected of DMH (40 mg/kg/bw) once a week for 12 successive weeks (de Paula Carli et al. 2012; Jia et al. 2014; Zhu et al. 2014). Group (5): DMH + ART group co-administrated DMH (40 mg/kg/bw) once a week for 12 weeks (de Paula Carli et al. 2012; Jia et al. 2014; Zhu et al. 2014) with ART at the same previous dose for 24 weeks (Lai and Singh 2006; Boareto et al. 2008; Farombi et al. 2014; Patyar et al. 2017). Group (6): DMH + ART-PLA NPs group co-administrated DMH at the same previous dose (de Paula Carli et al. 2012; Jia et al. 2014; Zhu et al. 2014) with ART-PLA NPs at the same previous dose for 24 weeks (Lai and Singh 2006; Boareto et al. 2008; Farombi et al. 2014; Patyar et al. 2017) as mentioned in Fig. 1.

Blood and colon tissue sampling

After 24 weeks (12 weeks after the last DMH injection), all animals were anesthetized using mild ether anaesthesia and blood samples were collected from the retro-orbital plexus using heparinized capillary tubes. Then the blood was kept at room temperature for coagulation before being rotated in a cooling centrifuge at 3000 rpm for 10 min. The upper clear serum layers were collected and kept at − 80 °C. Rats were dissected after euthanization and the colon and rectum were removed, cleaned in ice-cold isotonic saline, opened longitudinally and examined for any gross abnormalities. Colon divided into three parts: the first part was immersed in a triazole reagent and kept at − 80 °C for qRT-PCR, the second part was kept in phosphate-buffered saline

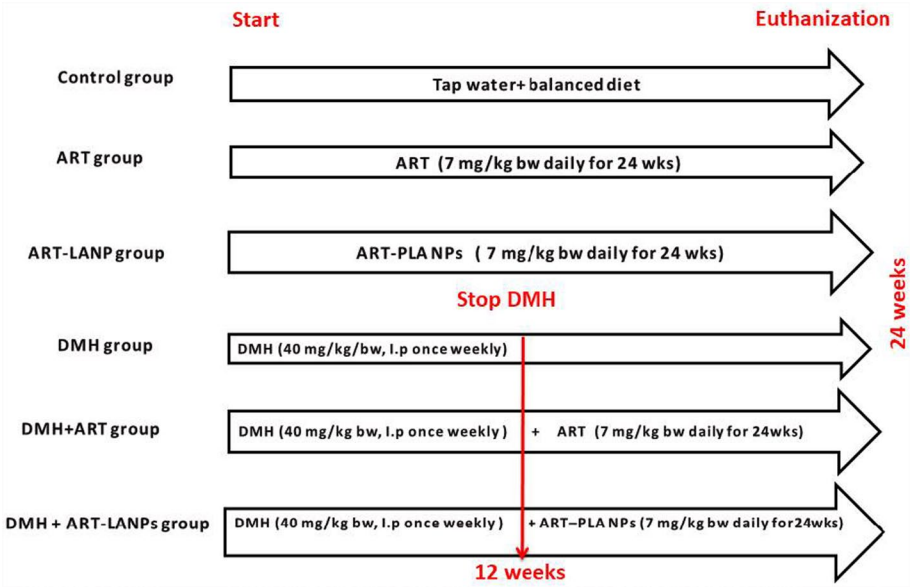

Fig. 1 Schematic representation of experimental design

containing protease inhibitor, the third part was kept in 10% neutral buffered formalin as a fixative for histopathological examination.

Assessment of serum level of carcinoembryonic antigen (CEA)

Assessment of serum CEA level was accomplished using a sandwich ELISA kit following manufacturer's protocols (Mohamed et al. 2022).

Assessment of colonic proinflammatory and anti-inflammatory cytokines

Colonic tissue protein levels of TNF-α, IL-1β, NF-kB-p65, and IL-10 were performed using ELISA kits. Phosphate-buffered saline (1× PBS, pH 7.4) with protease inhibitor was used for the colon samples preparation and the analysis was done according to the manufacturer's protocol (Khan et al. 2018).

Histopathological examination

The collected colon and rectum segments were dissected, preserved immediately in 10% neutral buffered formalin for fixation. After 24 h, the specimens were washed, dehydrated by ascending series of ethyl alcohol, dipped in xylene for clearance then paraffinized forming paraffin blocks. Next, the paraffin blocks were cut into 3–5 µm thick sections followed by deparaffinization and staining by hematoxylin and eosin for microscopical examination (Slaoui and Fiette 2011; Saini et al. 2012). The histopathological score was calculated as a sum of inflammation score (0–3), mucosal necrosis score (0–3), crypt damage score (0–3) and submucosal edema score (0–3) m (Pai et al. 2018).

Alcian blue staining

Alcian blue staining was used to identify the depletion of mucin in DMH goblet cells. In short, the deparaffinized sections were stained for 30 min with 1% alcian blue after

being immersed in 3% acetic acid for 2 min. After washing and five minutes of neutral red staining, the slices were rehydrated with alcohol, mounted, and seen under a light microscope (Shree et al. 2020, 2022). The percentage of goblet cells area was quantified using "Image J" software (Babu et al. 2023).

Masson's trichrome staining

Masson's trichrome staining was performed for detection of collagen fibers deposition in all experimental groups. Deparaffinized slides were fixed in Bouin's solution after being immersed in distilled water. Next, the sections were dipped in Weigert's hematoxylin stain, Biebrich scarlet acid fuchsin then in phosphomolybdic–phosphotungstic acid solutions for differentiation. After that, Fast Green was used for staining the sections then examined under light microscope (Sayed et al. 2023). The percentage of fibrosis area % was quantified using "Image J" software (El-Kholy et al. 2021; Babu et al. 2023).

RNA isolation and real-time polymerase chain reaction (RT-PCR) analysis

Total RNA was manually extracted from 100 mg of colon tissue in TRIZOL reagent using a handheld homogenizer to homogenize the tissue. A nanodrop spectrophotometer was employed to quantify the extracted RNA samples. Then the complementary DNA (cDNA) strand was synthesized using cDNA synthesis kits. The total reaction mixture was carried out at a volume of 20 µl: 4 µl total RNA, 4 µl 5 × TransAmp buffer, 1 µl reverse transcriptase and 11 µl DNase-free water. The thermal cycler temperature program was 50 °C reverse transcription for 30 min. The rat *β-actin*, *β-catenin*, and *adenomatous polyposis coli* (*APC*) primers sequences were designed and verified using Primer Blast NCBI (Table 1). SYBR Green master mix and the primers were employed for amplification of the synthesized cDNA. The housekeeping gene β-actin acted as a reference for cDNA levels normalization. The total reaction mixture was carried out in 20 µl: 10 µl 2 × SensiFast SYBR, 2 µl cDNA, 1 µl of each primer, and 6 µl RNase free water. The PCR cycling conditions were 94 °C primary denaturation for 15 min followed by 40 cycles of 94 °C secondary denaturation for 15 s, 60 °C annealing temperature for 30 s and 72 °C extension for 15 s. The gene expression difference among the experimental groups was analysed using $2^{-\Delta\Delta CT}$ method (Alkhuriji et al. 2021; dos Santos Cruz et al. 2022).

Western blotting analysis

The protein level of β-catenin and APC in the colonic tissue of all experimental groups was determined via western blotting. The protein extracted from colon tissue samples via homogenization in ice-cold RIPA lysis buffer. Followed by centrifugation of the homogenate at 10 000*g* for 10 min at 4 °C and collection of the clear supernatant

Table 1 Primer sequence of rat *β-actin*, *β-catenin*, and *adenomatous polyposis coli* (*APC*) genes analyzed by real-time polymerase chain reaction (RT-PCR)

Primer	Sense (5′–3′)	Antisense (5′–3′)	Size (bp)	Accession number
APC	ATGCACGGGCTCACTGATGA	GTGCCCTCATGCAGCCTTTC	133	012499.1
β-Catenin	GCGGCTGCTGTTCTATTCCG	TCTCCCTGGGCACCAATGTC	152	053357.2
β-actin	CCCCTCTGAACCCTAAGGCCA	CCAGTGGTACGACCAGAGGC	127	031144.3

as a prepared lysate. The concentration of the protein in the total lysate was estimated depending on Bradford method (Bradford 1976). 30 µg of the extracted protein was loaded onto SDS–PAGE gel then the protein transferred to nitrocellulose membrane that blocked by skimmed milk. Next, the membrane incubated overnight with primary antibodies against β-catenin, APC and β-actin then subjected to 2 h incubation with horseradish peroxidase (HRP)-conjugated secondary antibodies. The signals were detected using chemiluminescence (ECL) substrate, then the bands intensity quantification accomplished by Image J software (Rajendran et al. 2024).

Statistical analysis

The obtained results were quantitatively analyzed by one-way ANOVA followed by Tukey's adjustment test to compare all means using the GraphPad Prism software, p-value < 0.05 was considered statistically significant.

Results

Preparation and characterization and encapsulation efficiency of ART-Loaded PLA NPs

ART-loaded PLA nanoparticles were successfully prepared using the emulsion-solvent evaporation technique. The prepared nanoparticles were homogenous and spherical in shape with a particle size ranged from 40 to 50 nm (Fig. 2). Moreover, the encapsulation efficiency (EE%) of ART-loaded PLA nanoparticles was 84.5% calculated from the mentioned equation.

Effect of ART and ART-PLA NPs on serum level of carcinoembryonic antigen (CEA)

The obtained result demonstrated a significant increase in serum CEA concentration in DMH group in comparison to control group (Fig. 3). In contrast, it significantly decreased in DMH + ART group in comparison to DMH group. Additionally, DMH + ART-PLA NPs group revealed a more significant reduction in comparison to DMH group, but still showed no significant elevation in comparison to control group.

Effect of ART and ART-PLA NPs treatment on colonic inflammatory markers

DMH group revealed more significant increase in TNF-α, NF-κB and IL-1β beside more significant decrease in IL-10 colonic tissue contents in comparison to control group.

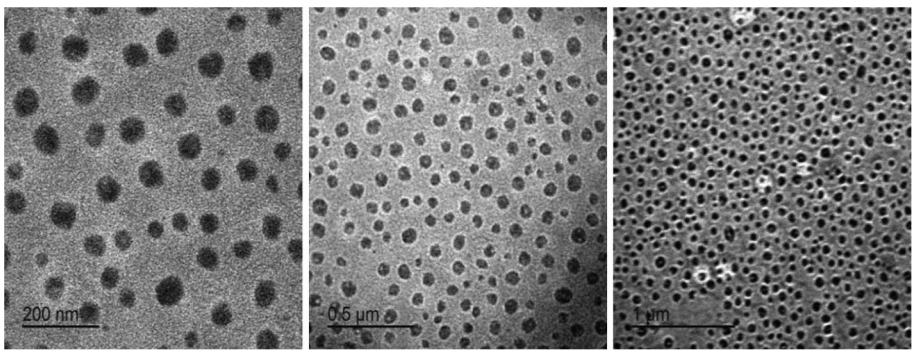

Fig. 2 Transmission electron micrographs of artemisinin-loaded polylactic acid nanoparticles (ART-PLA NPs) showing their homogenous and spherical shapes with a particle size ranging from 40 to 50 nm

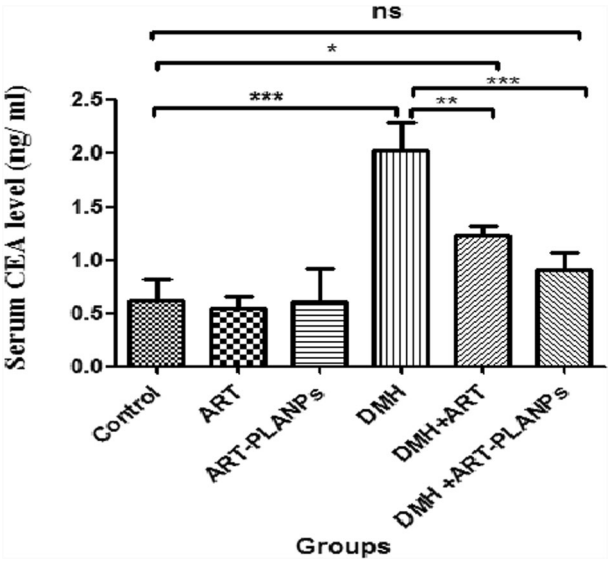

Fig. 3 Effect of artemisinin (ART) and artemisinin-loaded polylactic acid nanoparticles (ART-PLA NPs) on serum levels of the tumor marker carcinoembryonic antigen (CEA) in the studied groups. Data are shown as mean ± SEM. Statistically significant differences were observed by one-way ANOVA followed by Tukey's multiple comparisons test (***$p < 0.001$, **$p < 0.01$, *$p < 0.05$, ns = not significant)

Instead, both ART-PLA NPs and ART treatments showed significant decrease in the elevated levels of TNF-α, NF-κB and IL-1β along with significant increase in IL-10 colonic tissue contents compared to DMH group, but ART-PLA NPs showed more improvement in the all mentioned markers than free ART (Fig. 4).

Macroscopical observation

Our macroscopic analysis showed no tumor masses in colonic mucosa of control, ART, ART-PLA NPs groups, but multiple large-sized tumor masses arose from the colonic mucosa of DMH group, the largest one measured about 620 mm^3. Few and small tumor masses were observed in the colonic mucosa of DMH + ART, the largest one measured about 72 mm^3 and very few and small tumor mass were detected in colonic mucosa of DMH + ART-PLA NPs group, the largest one measured about 33 mm^3 (Fig. 5), along with reduced animal mortalities in both groups (Table 2).

Microscopic examination

Hematoxylin and eosin-stained colorectal sections from control, ART and ART-PLA NPs showed normal histological features of the mucosa, submucosa and muscular layers with normal mucosal cellular structure characterized by goblet cells rich epithelium. The colorectal tissue of untreated DMH group revealed deep mucosal necrosis reaching muscularis mucosa, many distorted crypts, moderate to severe dysplasia, submucosal edema with leukocytic cells infiltration. Colorectal tissues from DMH + ART-treated group showed superficial mucosal necrosis, fewer distorted&dysplastic crypts, decreased submucosal edema. ART-PLA NPs treatment was more powerful than ART as indicated by superficial mucosal necrosis, dilated crypts with mild dysplasia (Fig. 6).

Different types of colorectal tumors were detected after DMHexposure including: small polypoid tubular adenoma, pedunclated tubular adenoma, sessile tubular

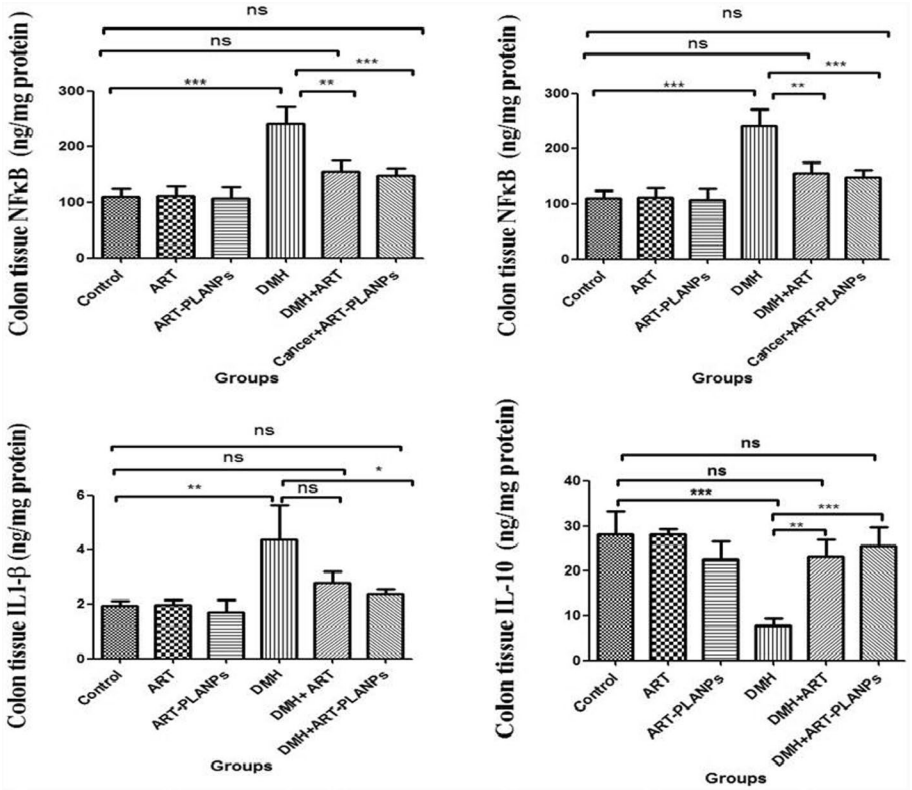

Fig. 4 Effect of artemisinin (ART) and artemisinin-loaded polylactic acid nanoparticles (ART-PLA NPs) on the colonic levels of the inflammatory markers NF-kB-p65, TNF-*α*, and IL-1β, and the anti-inflammatory marker IL-10 in the studied groups. Data are shown as mean ± SEM. Statistically significant differences were observed by one-way ANOVA followed by Tukey's multiple comparisons test (***$p < 0.001$, **$p < 0.01$, *$p < 0.05$, ns = not significant)

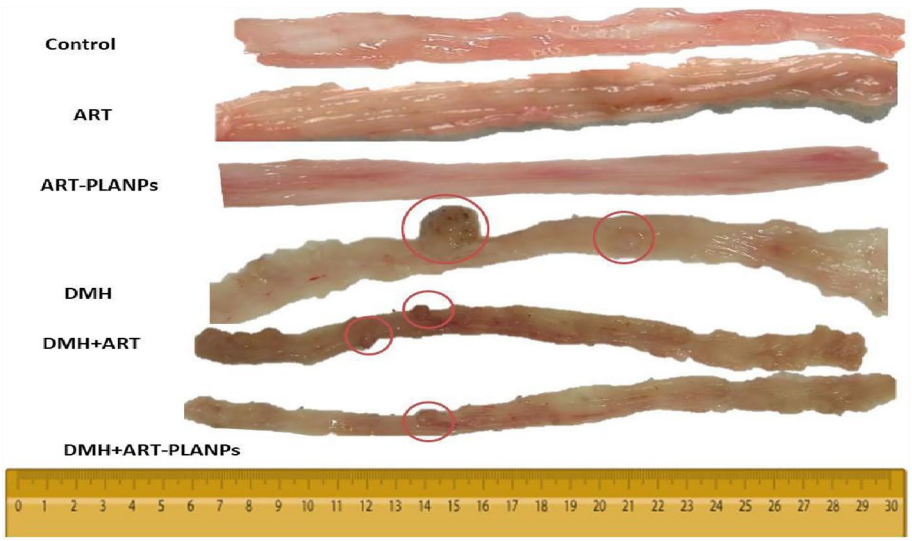

Fig. 5 Representative macroscopic pictures of the colonic mucosa showing the frequency of tumor masses (red circles) in the control, artemisinin (ART), and artemisinin-loaded polylactic acid nanoparticles (ART-PLA NPs) groups. Multiple large-sized tumor masses are present in the colonic mucosa of dimethylhydrazine (DMH) group; few and small tumor masses are seen in the colonic mucosa of DMH + ART group; and very few and small tumor masses are detected in colonic mucosa of DMH + ART-PLA NPs group

Table 2 Number of mortalities and tumor masses observed in dimethylhydrazine (DMH), DMH + artemisinin (DMH + ART), and DMH + ART-loaded polylactic acid nanoparticles (DMH + ART-PLA NPs) treated groups

Group	No. of animal /group	No. of mortality/group	No. of tumors/group
Control	10	–	–
ART	10	–	–
ART-PLA NPs	10	-	–
DMH	10	2	32
DMH + ART	10	1	17
DMH + ART-PLA NPs	10	–	12

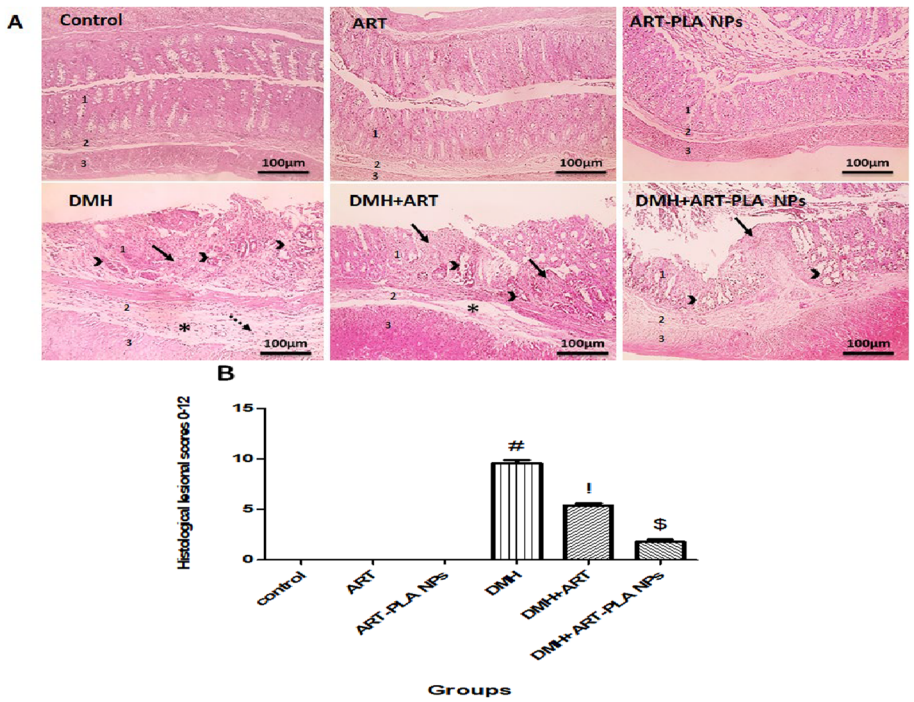

Fig. 6 **A** Representative microscopic pictures of H&E-stained sections of colorectal tissues from control, dimethylhydrazine (DMH), DMH + artemisinin (DMH + ART), and DMH + artemisinin-loaded polylactic acid nanoparticles (DMH + ART-PLA NPs) groups showing the histological features of the mucosa lined by an epithelium rich in goblet cells (1), the submucosa (2), and the muscularis (3). Colorectal tissue of DMH group reveals deep mucosal necrosis (black arrow) reaching muscularis mucosa, many distorted crypts with moderate to severe dysplasia (black arrowheads), and submucosal edema (*) with leukocytic cell infiltration (dashed black arrow). Colorectal tissue of DMH + ART group shows superficial mucosal necrosis (black arrow), fewer distorted crypts with moderate dysplasia (black arrowheads), and submucosal edema (*). Colorectal tissue of DMH + ART-PLA NPs group displays superficial mucosal necrosis (black arrow), dilated crypts (black arrowheads), and submucosal edema (*). Magnifications are × 100; bar = 100 µm. **B** Bar chart representing changes in total histological scores of colorectal tissue among various experimental groups. All the values are expressed as mean ± SEM ($n = 10$). # means significant as compared to control groups $p < 0.05$. ! means significant as compared to control groups and DMH group $p < 0.05$. $ means significant as compared to other groups $p < 0.05$

adenoma, tubulovillous and sessile serrated adenoma. The base of the adenoma was restricted to the colonic mucosa. Epithelial dysplasia was demonstrated in all tubular adenomas beside glandular overcrowding, hypercellularity, nuclear hyperchromasia with prominent nucleoli and increased mitotic figures. Atypical mitoses may be seen and the mucin production was generally depleted (Fig. 7A–E).

Masses that penetrate through the muscularis mucosa are malignant lesions further classified into: advanced adenocarcinomas (when the neoplastic cells invade submucosa through the muscularis mucosa), invasive adenocarcinoma (when tumors penetrate through the muscular layer). Histologically, adenocarcinomas were classified as: well-differentiated (when the cancer form uniform glandular structures with nuclei located at the basal half of the malignant cells), moderately differentiated (when the tumor composed of complex glandular structures and the nuclei loss their polarity) and poorly differentiated (when the cancer showed no to minimal gland formation). However, all the detected adenocarcinomas were moderately to poor differentiated. Mucinous adenocarcinomas (when cancer cells are suspended in mucous lakes). Signet ring adenocarcinoma characterized by presence of intracytoplasmic vacuoles

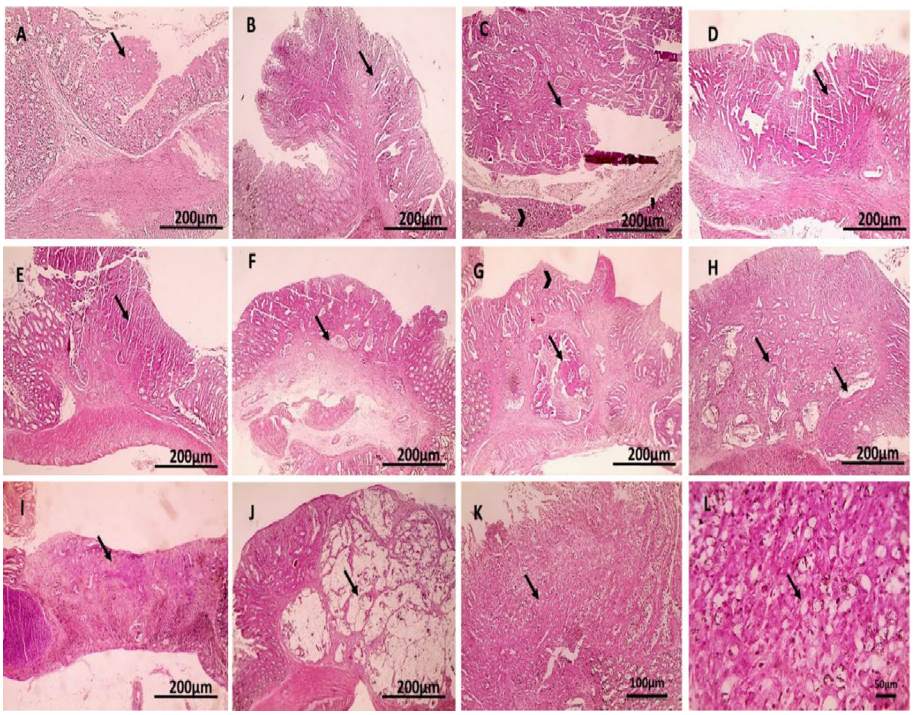

Fig. 7 Microscopic findings of H&E-stained colorectal tissues showing different types of colorectal tumors in all experimental groups including: small polypoid tubular adenoma (arrow) (**A**), pedunculated tubular adenoma (arrow) (**B**), sessile tubular adenoma (arrow), the base of the adenoma shows normal colonic mucosa (arrowhead) (**C**), tubulovillous adenoma (arrow) (**D**), sessile serrated (arrow) (**E**), advanced moderately differentiated adenocarcinomas in mucosa starts to infiltrate submucosa (arrow) (**F**), advanced moderately differentiated adenocarcinomas (arrow) in mucosa and deeply infiltrating submucosa (**G**), advanced moderately differentiated adenocarcinomas deeply infiltrating submucosa (arrow) with intact mucosa (arrowhead) (**H**), invasive poorly differentiated adenocarcinoma (arrow) reaching muscular layer and serosa (**I**), invasive mucinous adenocarcinoma (arrow) reaching muscular layer in some points **(J)** and signet ring adenocarcinoma (arrow) infiltrating submucosa (**K** and **L**). Magnifications are 40×, bar = 200, ×100, bar = 100 and 400×, bar = 50

Table 3 Types and numbers of colorectal tumors observed in dimethylhydrazine (DMH), DMH + artemisinin (DMH + ART), and DMH + ART-loaded polylactic acid nanoparticles (DMH + ART-PLA NPs) treated groups

	Polypoid tubular adenoma	Polypoid tubulovillous adenoma with dysplasia	Sessile villous adenoma	Sessile tubular adenoma	Sessile serrated adenoma	Advanced tubular adenocarcinoma	Invasive poorly differentiated adenocarcinoma	Mucinous advanced adenocarcinoma	Signet ring advanced adenocarcinoma
DMH	4	6	2	2	2	9	5	1	1
DMH + ART	3	3	2	1	1	3	2	1	1
DMH + ART-PLA NPs	2	3	1	1	1	2	2	0	0

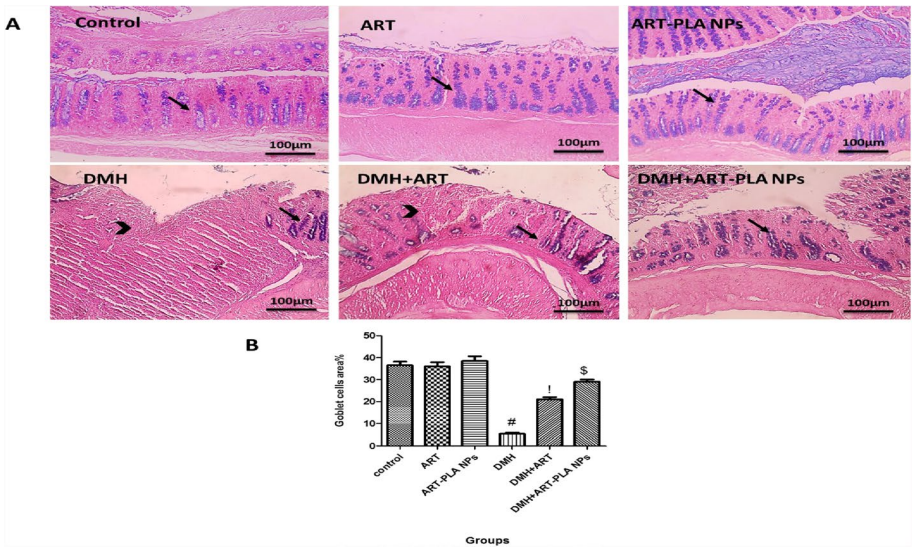

Fig. 8 **A** Representative microscopic pictures of alcian blue-stained colorectal tissues from control, dimethylhydrazine (DMH), DMH + artemisinin (DMH + ART), and DMH + artemisinin-loaded polylactic acid nanoparticles (DMH + ART-PLA NPs) groups showing normal bluish mucous content in mucosal epithelium (black arrows). Colorectal tissue of DMH group reveals decreased mucous content in area of deep mucosal necrosis (black arrowheads). Colorectal tissue of DMH + ART group shows superficially decreased mucous content in mucosa (black arrowheads). Colorectal tissue of DMH + ART-PLA NPs group displays increased mucous content in the mucosa (black arrow). Somewhat increased goblet cell area (black arrow) with superficially decreased bluish mucous content in mucosa (black arrowheads). Colorectal tissue of DMH + ART-PLA NPs group showing markedly increased goblet cell area (black arrow). Magnifications are × 100; bar = 100 µm. **B** Bar chart representing changes in goblet cells area % in colorectal tissue using "Image J" software. All the values are expressed as mean ± SEM ($n = 10$). # means significant as compared to control group $p < 0.05$, ! means significant as compared to control groups and DMH group $p < 0.05$, $ means significant as compared to other groups $p < 0.05$

in neoplastic cells that cause peripheral displacement and compression of nuclei (Fig. 7F–L).

Number and size of colorectal tumors decreased in DMH + ART group. ART-PLA NPs treatment was more powerful as indicated by fewer and smaller tumor masses. Type and number of colorectal tumors in all experimental groups are demonstrated in Table 3.

Effect of ART and ART-PLA NPs treatment on Alcian blue staining

Microscopic examination of Alcian blue-stained colorectal sections showed normal mucous secretion in colorectal section from normal control, ART and ART-PLA NPs groups. A marked reduction of mucous secretion was observed in mucosa of colorectal sections from untreated DMH group. Only superficially decreased bluish mucous content was seen in mucosa of colorectal sections from DMH + ART group. Higher mucous secretion was seen in mucosa of colorectal sections from DMH + ART-PLA NPs group (Fig. 8).

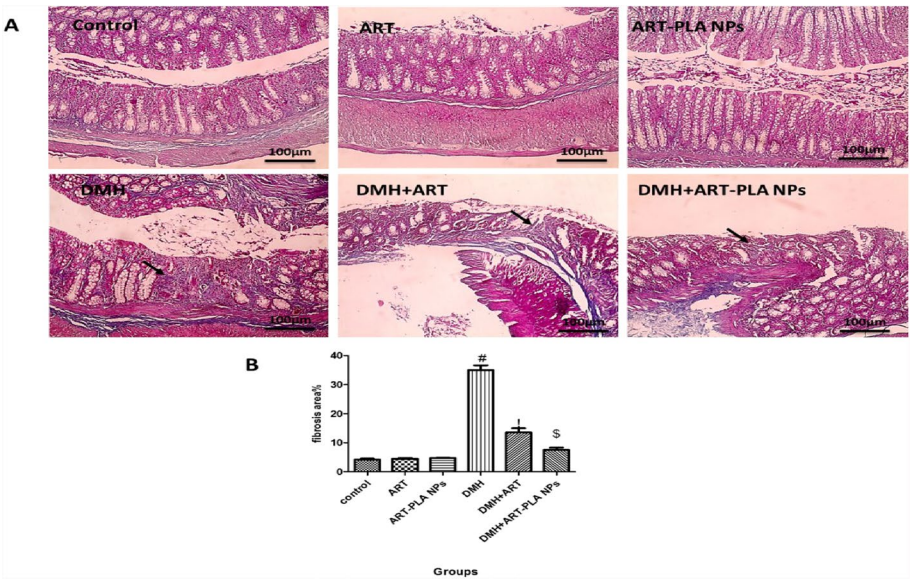

Fig. 9 **A** Representative microscopic pictures of Masson`s trichrome-stained colorectal tissues from control, dimethylhydrazine (DMH), DMH + artemisinin (DMH + ART), and DMH + artemisinin-loaded polylactic acid nanoparticles (DMH + ART-PLA NPs) groups showing the degree of mucosal fibrosis. Colorectal tissue of untreated DMH group revealing bluish mucosal fibrosis (black arrows). Colorectal tissue of DMH + ART group showing decreased bluish mucosal fibrosis (black arrows). Colorectal tissue of DMH + ART-PLA NPs group showing mild bluish mucosal fibrosis (black arrows). Magnifications are × 100; bar = 100 µm. **B** Bar chart representing changes in fibrosis area % in colorectal tissue. All the values are expressed as mean ± SEM ($n = 10$). #, significant as compared to control groups $p < 0.05$, ! means significant as compared to control groups and DMH group $p < 0.05$, and $ means significant as compared to DMH and DMH + ART groups $p < 0.05$

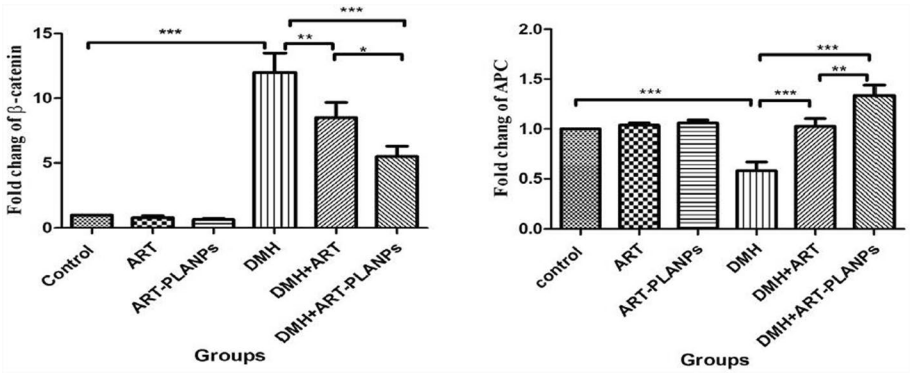

Fig. 10 Effect of artemisinin (ART) and artemisinin-loaded polylactic acid nanoparticles (ART-PLA NPs) on gene expression of *β-catenin* and *adenomatous polyposis coli* (*APC*) in the colonic tissues of the studied groups. Statistical differences were analyzed using one-way ANOVA followed by Tukey's multiple comparisons test (***$p < 0.001$, **$p < 0.01$, *$p < 0.05$)

Effect of ART and ART-PLA NPs treatment on Masson's trichrome staining

Microscopic examination of Masson`s trichrome-stained colorectal sections showing no fibrosis in any colorectal section from normal control, ART and ART-PLA NPs groups. Marked mucosal fibrous tissue deposition was detected in colorectal sections from untreated DMH group. Mucosal fibrous tissue deposition decreased in

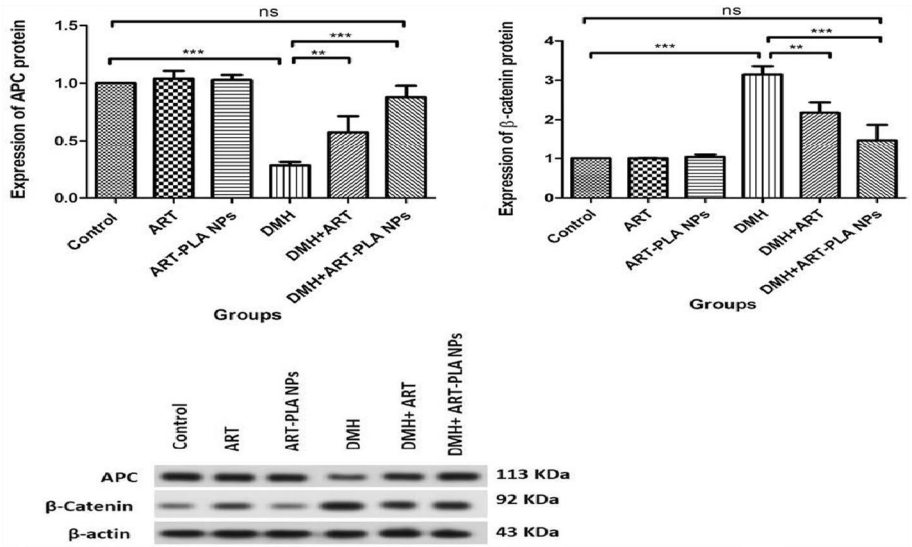

Fig. 11 Effect of artemisinin (ART) and artemisinin-loaded polylactic acid nanoparticles (ART-PLA NPs) on western blot analysis of β-catenin and adenomatous polyposis coli (APC) protein expression in the colonic tissues of the studied groups against β-actine as housekeeping protein and quantitative densitometry of their expression level. Statistical differences were analyzed using one-way ANOVA followed by Tukey's multiple comparisons test (***$p < 0.001$, **$p < 0.01$, *$p < 0.05$)

colorectal tissue from DMH + ART group. Mild mucosal fibrous tissue deposition was observed in colorectal tissue from DMH + ART− PLA NPs group (Fig. 9).

Effect of ART and ART-PLA NPs treatment on β-Catenin and APC gene expression

The expression level of *β-catenin* gene in the colon of DMH group showed significant increase in *β-catenin* expression, followed by the DMH + ART group, then the DMH + ART-PLA NPs group. No significant differences were found among the other remaining groups. Meanwhile, the expression levels of *APC* gene in the colon of DMH group was significantly lower than other groups. On the other hand, DMH + ART-PLA NPs group was significantly higher than other groups. There was no significant difference among the remaining groups (Fig. 10).

Effect of ART and ART-PLA NPs treatment on western blot analysis of β-Catenin and APC protein expression

As demonstrated in Fig. 11, there were significant increase in β-Catenin protein expression level and marked decrease in APC expression in DMH-induced group compared to the control group. Instead, ART and ART-PLA NPs treatment could significantly decrease β-Catenin level and increase the APC protein levels when compared to DMH group. ART-PLA NPs was able to downregulate the expression of β-Catenin and increase expression of APC noticeably almost near to the control group.

Discussion

Colorectal cancer (CRC) took the third position among the most dangerous malignant neoplasms worldwide (Xi and Xu 2021). Side effects and drug resistance caused by modern treatments like radiation and chemotherapy made the development of safe and effective anticancer drugs is a major challenge. In this context, nanomedicine formulation from the natural products provides safe and effective chemoprotective approach preventing CRC early lesions progression (Sharma et al. 2018; Mata et al. 2023). The safe toxicity profile of ART and its derivatives made them more attractive for the research. ART and its based compound recorded potent and broad anticancer properties against many human cancer cell lines and animal models (Krishna et al. 2008; Ho et al. 2014; Efferth 2017), such as breast cancer (Wen et al. 2018), ovarian, liver (Zhou et al. 2021), prostate (Zhou et al. 2017), oral cancer cells (Nam et al. 2007), pancreatic cancer (Zhou et al. 2013) and colorectal cancer (Li et al. 2020a, b; Lin et al. 2021). ARTs target the cancer cells by several mechanisms including cell cycle regulation, induction of apoptosis or hindering proliferation and downregulation of hyperactive Wnt/β-catenin signaling pathway. Moreover, they suppressed tumor invasion and metastasis through inhibition of angiogenesis-related mediators (Efferth 2007, 2017; Krishna et al. 2008; Xu et al. 2020; Ho et al. 2014). ART still has some drawbacks, including poor solubility in water and oil, low bioavailability, initial burst effect in vivo that identified by high peak plasma concentrations and accelerated metabolism (Chen et al. 2009; Zeng et al. 2023). Therefore, this investigation tried to enhance the anticancer efficacy of ART by loading it into polylactic acid nanoparticles (ART-PLA NPs) and investigated its ameliorative effect against 1.2 *N*,*N*-dimethylhydrazine (DMH) induced CRC through targeting wnt/β-catenin and NF-κB pathways.

The encapsulation efficiency is an important parameter that explains the validity of PLA nanoparticles formulation. Our result showed that the EE% was 84.5% which indicated good affinity of the drug to PLA nanoparticles, improved the delivery of the drug dosage and confirmed the efficiency of ART nanoformulation as mentioned in previous report (Tran et al. 2017; Fattahi and Zamani 2022).

Tumor markers are biological substances that are either synthesized by cancer cells or being formed in reaction related to the presence of tumor tissue or circulating tumor cells in bone marrow, lymph nodes, serum, and peripheral blood. Tumor marker described as a chemical that suggests the possibility of cancer or offers details on how a malignancy is likely to behave in the future (Malati 2007). Carcinoembryonic antigen (CEA) is one of the most commonly estimated tumor marker and frequently used in colorectal cancer diagnosis (Nakatani et al. 2012). Our data revealed that serum CEAconcentration was significantly increased upon DMHexposure in comparison to the control group, owing to colon cancer induction and increase the number of malignant cells and their production. These data are in agreement with other previous studies concerned with colon cancer (Hassan et al. 2021; Vural et al. 2023). In contrast, serum CEA concentration showed significant decrease upon DMH + ART and DMH + ART-PLA NPs coadministration in comparison to the DMH group. As the results in this context concerned with ART and its nanoformulation are limited, we found that these results in agreement with other previous study that evaluated the anticancer effect and tolerability of oral artesunate, (ART derivative), in colorectal cancer and noticed ~ 75% fall in circulating CEA levels

after 2 weeks of treatment (Krishna et al. 2015). Our result reflected the anticancer activity of ART and ART-PLA NPs which explained by the reduction in the malignant cells with decrease CEA release. Additionally, the more reduction in CEA concentration after ART-PLA NPs administration may be attributed to the improvement in the bioavailability and targetability of ART after its nanoformulation.

Inflammation is considered one of the early lesions affecting the colorectal mucosa in the course of chemicals-induced carcinogenesis. Inability of the immune system to overcome the injury leads to elevate the concentration of cytokines, growth factors, and products of cellular respiration resulting in persistent proliferation of genetically defected cells (Mariani et al. 2014). In the tumor microenvironment, inflammatory cytokines control tumor-stromal cell communication and tumor-extracellular matrix interactions, which in turn promote tumor growth (Balkwill and Mantovani 2001). Nuclear factor κB (NF-κB) NF-KB is a family of important transcription factors consists of five proteins namely, c-Rel, RelB, P52, P50 and P65.In resting condition, these proteins sequestered in the cytoplasm forming homodimers or heterodimers complexes holding with inhibitor of NF-KB (IkB). IkB kinases (IKK) is a key inducer of NF-κB signaling pathway. Its activation leads to IkB phosphorylation and ubiquitin-dependent proteasome degradation (Lin and Yang 2018). In the tumor microenvironment, TNFα, IL-1β, IL-6 and other inflammatory cytokines, the main drivers of NF-κB, could stimulate NF-κB pathway through IKK activation (Klampfer 2011; Patel et al. 2018; Zhao et al. 2020). Leads to phosphorylation and proteasome degradation of IkB along with release of P50/P65 complex that undergoes nuclear translocation. The translocated P50/P65 complex interacts with its specific target genes promotes their expression and drives the cell proliferation, apoptosis, angiogenesis, invasion, and metastasis (Wang et al. 2020a; Gupta et al. 2023). Moreover, it was reported that NF-κB inhibition could promote cancer cell apoptosis through upregulation of caspase-3 and decreased levels of anti-apoptotic protein as mentioned in ovarian cancer cells (Yang et al. 2018). Additionally, previous studies demonstrated that activated NF-kB is recorded in different types of cancers, animal models xenograft and many cancer cell lines triggering chemotherapy resistance. Activated NF-kB was reported in about 40% of human CRC cases and in 66% of CRC cell lines (Sakamoto et al. 2009; Voboril and Weberova-Voborilova 2006). Therefore, NF-κB signaling pathway is considered an important target for cancer therapy.

Our study showed direct evidence of more significant increase in the colonic tissue content of TNF-α, NF- κB, and IL-1β along with more significant decrease in IL-10 upon DMH exposure. These data are in agreement with Khan et al. (2018), Shree et al. (2022). On the other hand, the elevated levels of TNF-α and IL-1β revealed more significant decrease upon ART-PLA NPs treatment which reflected on the level of NF- κB. Consequently, our collected data revealed that ART and ART-PLA NPs could modulate the inflammatory reaction against DMH carcinogenesis via suppression of NF-κB signalling pathway as stated in previous studies (Kumar et al. 2019; Efferth and Oesch 2021). It was reported that ART and its derivatives could supress NF-κB pathway though attenuation of TNF-α induced IkB phosphorylation and degradation, consequently inhibits P65 activation and nuclear translocation. As a result inhibition of NF-kB target genes expression along with other adaptor proteins as TNF receptor-associated factor 2 (TRAF2) and receptor interacting protein 1 (RIP1) leads

to upstream of Inhibitor of Nuclear Factor-Kappa B Kinase (IKK) signaling (Wang et al. 2017). Collectively, our formulated ART-PLA NPs suppress NF-κB pathway efficiently and this implemented in CRC treatment. As it could reduce cell proliferation and subsequent recorded decrease in the tumor marker, tumor number, size along and decrease the mortalities along with recorded improvement in the histopathological parameters.

Our histopathological study of colorectal tissue of untreated DMH group revealed deep mucosal necrosis reaching muscularis mucosa, many distorted crypts, moderate to severe dysplasia, submucosal edema with leukocytic cells infiltration. In accordance (Sadik 2013; Hassan et al. 2021), found irregular distorted crypts lined with dysplastic cells that invade deeply to the muscle layers and loss of mucous secretion along with mucosal ulceration. Colorectal tissues from DMH + ART-treated group showed superficial mucosal necrosis, fewer distorted and dysplastic crypts, and decreased submucosal edema. While ART-PLA NPs treatment was more powerful than ART as indicated by superficial mucosal necrosis and dilated crypts with mild dysplasia. These data are in agreement with other previous studies (Kumar et al. 2019; Yin et al. 2020; Hu et al. 2014) who demonstrated the ability of artemisinins to reduce the surface epithelial cells erosion, crypts destruction and the inflammatory cells infiltration in the colonic tissue.

In this study, different types of adenomas were detected upon DMH exposure including tubular, villous, and tubulovillous histological types with polypoid, pedunculated, and sessile serrated growth patterns that limited to mucosa. Epithelial dysplasia was demonstrated in all adenomas beside glandular overcrowding, hypercellularity along with mucin depletion. In addition to nuclear enlargement, hyperchromasia, prominent nucleoli, increased mitotic figures and atypical mitoses. These findings in accordance with previous studies (Hamilton and Aaltonen 2000; Cerar et al. 2004; Shojaei-Zarghani et al. 2020). Additionally, different types of adenocarcinomas were detected invading the submucosa and the muscular layers. All observed adenocarcinomas were moderately to poorly differentiated beside mucinous and Signet ring adenocarcinoma types. Our observations are in line with the previous studies (Boivin et al. 2003; Caetano et al. 2018, 2020; Mohammadzadeh et al. 2024). In contrast, we observed that the number and size of colorectal tumors decreased upon ART treatment. While ART-PLA NPs supplementation was more powerful as indicated by fewer and smaller tumor masses. These findings suggested the anticancer properties of ART which enhanced after its nanoformulation in accordance with previous reports (Li et al. 2020a, b; Wang et al. 2020a, b; Wen et al. 2024) who confirmed the antiproliferative effects of ART and its derivatives through inducing apoptosis and cell cycle arrest. In addition to their ability to hider the inflammatory reaction and subsequent tumor formation and increasing CD8+ T cell infiltration (Bai et al. 2021; Sun et al. 2023).

The goblet cells distributed among the epithelial lining of the colonic crypts play important role in the protection of the colonic mucosal surface through the mucous secretion forming a gel-like coat that protects and maintains the integrity of colonic surface (Johansson and Hansson 2016). Previous reports demonstrated that the distal part of colon in healthy rats and humans normally secretes sulfomucin meanwhile, sialomucin is the predominant type found in colon cancer patients and DMH-induced rats (Tanaka 2009; Shree et al. 2020, 2021). Our results showed marked reduction of mucin

production upon DMH administration that may attributed to its ability to destruct goblet cells in colon tissues leading to decrease the production of specific mucin such as MUC2 and shift normal sulphomucin to sialomucin as stated in the previous reports (Kumar and Agnihotri 2021; Shree et al. 2020, 2022). On the other hand, our findings confirmed the protective role of ART and ART-PLA NPs in maintaining goblet cells integrity and restoring the mucous secretion. As there were only superficial decrease in the bluish mucous content upon ART administration and higher bluish mucous content in the mucosa after ART-PLA NPs supplementation. This result in accordance with (Yin et al. 2020) who clarified the ability of ART-based medication to protect the mucosal barrier via inhibition the reduction of Muc2 and claudin-1 in dextran sulphate sodium induced ulcerative colitis.

In the present study, masson trichrome stained colon sections revealed marked mucosal collagen fiber deposition upon DMH administration. This was in accordance with (Alkhuriji et al. 2021; El-Kholy et al. 2021). Whereas treated groups with ART and ART- PLANPs showed mild mucosal collagen fiber deposition. This explained the ability of ART and its derivatives to diminish the inflammation with subsequent decrease fibrosis through inhibition of Transforming growth factor beta (TGF-β) signaling. Moreover, ART could enhance M1 macrophage to M2 macrophage polarization, resulting in regression of the pro-inflammatory mediators and supressed the epithelial-mesenchymal transition (Huai et al. 2021) as mentioned in gastric cancer cells (Li et al. 2019), ovarian cancer cells (Liang et al. 2019), and renal fibrosis (Zhang et al. 2019). Additionally, they could inactivate cancer associated fibroblasts proliferation as reported in breast cancer model and they were able to inhibit TGF-β signalling pathway (Yao et al. 2018).

The Wnt/β-catenin cell signalling pathway is considered as a crucial pathway in the development of CRC. β-catenin is the principal controlling protein in this pathway (Zhang and Wang 2020). In normal condition and absence of Wnt ligands, cytoplasmic β-catenin is rapidly subjected to phosphorylation, ubiquitination then proteasome degradation through binding with its destruction complex, including adenomatous polyposis coli (APC), Casein kinase 1 (CK1), Axin and Glycogen Synthase Kinase (GSK3β) (Nusse and Clevers 2017). Colon carcinogenesis is frequently associated with mutations, attenuation of gene expression or deletion of Wnt/β-catenin related main components as β-catenin, APC or Axin hindering β-catenin degradation. Subsequently cytoplasmic accumulation and nuclear translocation of β-catenin. In the nucleus, β-catenin combines with T-cell factor and lymphoid enhancer factor 1 to control the transcription of several oncogenes affecting cell proliferation and differentiation (Schaefer and Peifer 2019). Additionally, several studies either clinical or experimental operated on rats or human cancer cell lines have shown that APC loss is the main driver of Wnt/β-catenin pathway during colon carcinogenesis. As it recorded in about 70% of sporadic CRC and is considered the main suspect of familial adenomatous polyposis (FAP) (Kim and Jeong 2019; Sansom et al. 2007). Moreover, it was recorded that, restoration of APC could restore tissue homeostasis and prevent recurrence of CRC through enhancement of tumor cell differentiation and inverse *C*-MYC-induced oncogenic state (Dow et al. 2015). Unregulated Wnt/β-catenin pathway leads to targeting many genes encouraging cancer cell proliferation, apoptosis evasion, invasion, angiogenesis and metastasis (Song et al. 2019; Ten Berge et al. 2011). Therefore, in this study we aimed to investigate the role of ART and

ART-PLA NPs in regulation the Wnt/β-catenin pathway as an important molecular target during CRC carcinogenesis.

In this study, it is important to highlight the significant increase in *β-catenin* gene and its related protein expression in the DMHgroup, followed by the DMH + ART group, then DMH + ART-PLA NPs group that revealed more pronounced decrease almost near to the control group. Coinciding with our findings, (Yu et al. 2017) reported the upregulation of *β-catenin* expression in DMHinduced CRC. The upregulation of *β-catenin* is a well-established feature in the initiation and evolution of CRC (Schaefer and Peifer 2019) and the pattern seen in this study supports its relevance as a potential biomarker and therapeutic target in colon cancer research. In contrast, the expression level of the *APC*gene and its related protein in the colon were observed to be significantly lower in the DMHgroup compared to the other groups. While the DMH + ART-PLA NPs group showed significantly higher *APC*gene and protein expressions than the other groups. These findings are consistent with the results reported by (Sadik and Shaker 2013) who demonstrated the downregulation of *APC*expression in the colonic tissues of DMH-induced colon cancer. Also, our findings suggested that ART-PLA NPs may help counteract the loss of *APC*expression, resulting in β-catenin degradation and inhibition of its target genes expression. Consequently, this implicated in its anti-proliferative efficacy against CRC as it decrease the reported tumors number, types, size and improved the colonic histopathological picture. Additionally, the observed attenuation of the hyperactive Wnt/β-catenin related genes after ART and DMH + ART-PLA NPs treatment was supported by previous studies (Li et al. 2007; Zheng and Pan 2018). One study demonstrated that ART could regulate Wnt/β-catenin pathway through translocation the nuclear β-catenin to the adjacent membrane junctions leading to reduce β-catenin target gene transcription (Li et al. 2007). But another study recorded that ART and its derivatives could inhibit Wnt/β-catenin pathway during lung carcinogenesis through reduction of Wnt5-a/b protein level and subsequent increase in Axin2 and NKD2 levels leading to downregulation of β-catenin (Tong et al. 2016).

In our study, we recorded absence of mucinous and signet ring adenocarcinomas in ART-PLA NPs treated group. Signet ring adenocarcinoma is a very aggressive and invasive subtype with poor prognosis. It differs from the conventional adenocarcinoma, as it has lower mutation rate of RAS/RAF/MAPK, Wnt/β-catenin and PI3K/AKT/mTOR pathways. Instead, it exhibited frequent mutation in *CDH1* gene that encodes E-cadherin also other genes connected to TGF-β and epithelial-mesenchymal transition (EMT) process (An et al. 2021). Therefore, restoring E-cadherin expression and inhibition of TGF-β and EMT process may be possible therapeutic approach for treating this subtype. In our study, ART-PLANPs may target this subtype indirectly through regulation of Wnt/β-catenin pathways or by another signaling pathways as mentioned in previous studies (Li et al. 2008; Weifeng et al. 2011). In the same way, mucinous adenocarcinoma associated with activation of PI3K/AKT pathway and exhibited more TGF-β mutations than conventional adenocarcinoma (Haque and Morris 2017; Vivanco and Sawyers 2002; Lan et al. 2021). Therefore, targeting these pathways may be suitable therapeutic approach. Our treatment may regulate these pathways and could inhibit the development of such subtype as mentioned in previous studies (Wang et al. 2020b; Wu et al. 2020; Li et al. 2020b), so this point need further investigation.

Limitations

Although ART-PLA NPs targeted the colorectal cancer through two main mechanisms namely, NF-κB and Wnt/β-catenin signaling pathways, there are many pathways need further investigation to confirm and clarify the therapeutic potential of ART-PLA NPs. Second, dose dependent study would be beneficial to determine the effective dose ART-PLA NPs. Moreover, limited in vitro study using CRC cell line. And finally limited pharmacokinetic data about the ART nanoformulation. Therefore, these points need further investigation.

Conclusion

In conclusion, ART-PLA NPs appeared more powerful than ART as indicated by lower serum tumor marker and targeting NF-κB signaling pathway through lower levels of colonic tissues inflammatory cytokines. In addition to absence of mortalities, fewer and smaller tumor masses with macroscopic investigation along with increase the protective mucus secretion and mild mucosal fibrosis by histological examination. Additionally, it could control cell proliferation through targeting Wnt/β-catenin pathway as it exhibited downregulation of hyperactive *β-catenin* gene and related protein expression and demonstrated upregulation of *APC* gene and related protein expression. Thus it could be considered as a new prophylaxis strategy against colon cancer in the clinical fields.

Abbreviations

AOM	Azoxymethane
APC	*Adenomatous Polyposis Coli*
ART	Artemisinin
cDNA	Complementary DNA
CEA	Carcinoembryonic antigen
CK1	Casein kinase 1
CRC	Colorectal cancer
DMH	Dimethylhydrazine
ELISA	Enzyme-Linked Immunosorbent Assay
EMT	Epithelial–mesenchymal transition
FAP	Familial adenomatous polyposis
GSK3β	Glycogen Synthase Kinase
IKK	Inhibitor of Nuclear Factor-Kappa B (IκB) Kinase
IL-10	Interleukin 10
IL-1β	Interleukin 1 beta
MAM	Methylazoxymethanol
MERC	Medical Experimental Research Center
NF-κB	Nuclear factor kappa B
PLA	Polylactic acid
PLA NPs	Polylactic acid nanoparticles
PVA	Polyvinyl alcohol
RIP1	Receptor interacting protein 1
RT-PCR	Real-time polymerase chain reaction
TEM	Transmission electron microscope
TGF-β	Transforming growth factor beta
TNF-α	Tumor necrosis factor-α
TRAF2	TNF receptor-associated factor 2

Acknowledgements

Not applicable.

Author contributions

All authors contributed to the research conception and design. Zeinab dwidar and Walaa F. Awadin: conceptualization, methodology, formal analysis, investigation, validation, writing the first draft of the manuscript and supervision. Mohamed El-Adl and Ahmed M. Abdellatif: conceptualization, methodology, writing the first draft of the manuscript, editing. Mohamed Abomosallam and Aya Aly Elzeer: methodology, reviewed, editing and commented on previous versions of the manuscript. All authors read and approved the final manuscript.

Funding
Open access funding provided by The Science, Technology & Innovation Funding Authority (STDF) in cooperation with The Egyptian Knowledge Bank (EKB).

Availability of data and materials
No datasets were generated or analysed during the current study.

Declarations

Ethics approval and consent to participate
This research was approved by the Ethical Committee, Faculty of Veterinary Medicine, Mansoura University, Egypt under code number (VM.phD.23.06.15).

Consent for publication
Not applicable.

Competing interests
The authors declare no competing interests.

Received: 10 January 2025 Accepted: 21 March 2025
Published online: 19 April 2025

References

Aderibigbe BA (2017) Design of drug delivery systems containing artemisinin and its derivatives. Molecules 22(2):323
Aggarwal B, Prasad S, Sung B, Krishnan S, Guha S (2013) Prevention and treatment of colorectal cancer by natural agents from mother nature. Curr Colorectal Cancer Rep 9(1):37–56
Alkhuriji AF, Alsaiari SG, Alomar SY, Alnafjan AA, Alobaid H, El-Khadragy MF (2021) Effect of mesenchymal stem cells on cytochrome-c release and inflammation in colon cancer induced by 1, 2-dimethylhydrazine in Wistar albino rats. Biosci Rep 41(3):BSR20204356
Allen TM, Cullis PR (2004) Drug delivery systems: entering the mainstream. Science 303(5665):1818–1822
Alzahrani SM, Al Doghaither HA, Al-Ghafari AB (2021) General insight into cancer: an overview of colorectal cancer (Review). Mol Clin Oncol 15(6):271
An Y, Zhou J, Lin G, Wu H, Cong L, Li Y, Qiu X, Shi W (2021) Clinicopathological and molecular characteristics of colorectal signet ring cell carcinoma: a review. Pathol Oncol Res 27:1609859
Appalasamy S, Lo KY, Ch'ng SJ, Nornadia K, Othman AS, Chan LK (2014) Antimicrobial activity of artemisinin and precursor derived from in vitro plantlets of *Artemisia annua* L. Biomed Res Int 1:215872
Ashley EA, White NJ (2005) Artemisinin-based combinations. Curr Opin Infect Dis 18(6):531–536
Babu SSN, Singla S, Jena G (2023) Role of combination treatment of aspirin and zinc in DMH-DSS-induced colon inflammation, oxidative stress and tumour progression in male BALB/c mice. Biol Trace Elem Res 201:1327–1343
Badshah SL, Ullah A, Ahmad N, Almarhoon ZM, Mabkhot Y (2018) Increasing the strength and production of artemisinin and its derivatives. Molecules 23(1):100
Bai B, Wu F, Ying K, Xu Y, Shan L, Lv Y, Gao X, Xu D, Lu J, Xie B (2021) Therapeutic effects of dihydroartemisinin in multiple stages of colitis-associated colorectal cancer. Theranostics 11(13):6225
Balkwill F, Mantovani A (2001) Inflammation and cancer: back to Virchow? Lancet 357(9255):539–545
Bilia AR, Piazzini V, Guccione C, Risaliti L, Asprea M, Capecchi G, Bergonzi MC (2017) Improving on nature: the role of nanomedicine in the development of clinical natural drugs. Planta Med 83(05):366–381
Boareto AC, Muller JC, Bufalo AC, Botelho GG, de Araujo SL, Foglio MA, de Morais RN, Dalsenter PR (2008) Toxicity of artemisinin [*Artemisia annua* L.] in two different periods of pregnancy in Wistar rats. Reprod Toxicol 25(2):239–246
Boivin GP, Washington K, Yang K, Ward JM, Pretlow TP, Russell R, Besselsen DG, Godfrey VL, Doetschman T, Dove WF, Pitot HC (2003) Pathology of mouse models of intestinal cancer: consensus report and recommendations. Gastroenterology 124(3):762–777
Bradford MM (1976) A rapid and sensitive method for the quantitation of microgram quantities of protein utilizing the principle of protein-dye binding. Anal Biochem 72(1–2):248–254
Brannon-Peppas L, Blanchette JO (2004) Nanoparticle and targeted systems for cancer therapy. Adv Drug Deliv Rev 56(11):1649–1659
Brenner H, Chen C (2018) The colorectal cancer epidemic: challenges and opportunities for primary, secondary and tertiary prevention. Br J Cancer 119(7):785–792
Buabeid MA, Arafa ESA, Murtaza G (2020) Emerging prospects for nanoparticle-enabled cancer immunotherapy. J Immunol Res 1:9624532
Caetano BFR, Tablas MB, Pereira NEF, de Moura NA, Carvalho RF, Rodrigues MAM, Barbisan LF (2018) Capsaicin reduces genotoxicity, colonic cell proliferation and preneoplastic lesions induced by 1, 2-dimethylhydrazine in rats. Toxicol Appl Pharmacol 338:93–102
Caetano BFR, Tablas MB, Romualdo GR, Rodrigues MAM, Barbisan LF (2020) Early molecular events associated with liver and colon sub-acute responses to 1, 2-dimethylhydrazine: Potential implications on preneoplastic and neoplastic lesion development. Toxicol Lett 329:67–79
Casalini T, Rossi F, Castrovinci A, Perale GA (2019) Perspective on polylactic acid-based polymers use for nanoparticles synthesis and applications. Front Bioeng Biotechnol 7:259

Cerar A, Zidar N, Vodopivec B (2004) Colorectal carcinoma in endoscopic biopsies; additional histologic criteria for the diagnosis. Pathol Res Pract 200(10):657–662
Chen Y, Lin X, Park H, Greever R (2009) Study of artemisinin nanocapsules as anticancer drug delivery systems. Nanomedicine 5(3):316–322
Cunningham D, Atkin W, Lenz HJ, Lynch HT, Minsky B, Nordlinger B, Starling N (2010) Colorectal cancer. Lancet 375:1030–1047
de Paula Carli A, de Abreu Vieira PM, Silva KTS, de Sá Cota RG, Carneiro CM, Castro-Borges W, de Andrade MH (2012) Bowman-Birk inhibitors, proteasome peptidase activities and colorectal pre neoplasias induced by 1, 2-dimethylhydrazine in Swiss mice. Food Chem Toxicol 50(5):1405–1412
Dekker E, Tanis PJ, Vleugels JL, Kasi PM, Wallace MB (2019) Colorectal cancer. Lancet 394(10207):1467–1480
Dos Santos Cruz BC, da Silva DV, Dias RS, Bernardes AL, de Paula SO, Ferreira CLdLF, Peluzio MDCG (2022) Synbiotic modulates intestinal microbiota metabolic pathways and inhibits DMH-induced colon tumorigenesis through c-myc and PCNA suppression. Food Res Int 158:111379
Dow LE, O'Rourke KP, Simon J, Tschaharganeh DF, van Es JH, Clevers H, Lowe SW (2015) Apc restoration promotes cellular differentiation and reestablishes crypt homeostasis in colorectal cancer. Cell 161(7):1539–1552
Efferth T (2007) Willmar Schwabe Award 2006: antiplasmodial and antitumor activity of artemisinin-from bench to bedside. Planta Med 73(04):299–309
Efferth T (2017) From ancient herb to modern drug: artemisia annua and artemisinin for cancer therapy. Semin Cancer Biol 46:65–83
Efferth T, Oesch F (2021) The immunosuppressive activity of artemisinin-type drugs towards inflammatory and autoimmune diseases. Med Res Rev 41(6):3023–3061
El-Kholy WB, Abdel-Rahman S, El F-NAE-H, Issa NM (2021) Effect of vitamin B17 on experimentally induced colon cancer in adult male albino rat. Folia Morphol 80:158–169
Farombi E, Adedara I, Abolaji A, Anamelechi J, Sangodele J (2014) Sperm characteristics, antioxidant status and hormonal profile in rats treated with artemisinin. Andrologia 46(8):893–901
Fattahi FS, Zamani T (2022) Poly (lactic acid) nanoparticles a promising hope to overcome the cancers. J Adv Biomed Sci 11:3791–3814
Fattahi FS, Khoddami A, Avinc O (2019) Poly (lactic acid)(PLA) nanofibers for bone tissue engineering. J Text Polm 7(2):47–64
Feng SS (2004) Nanoparticles of biodegradable polymers for new-concept chemotherapy. Expert Rev Med Devices 1(1):115–125
Feng C, Yuan X, Chu K, Zhang H, Ji W, Rui M (2019) Preparation and optimization of poly (lactic acid) nanoparticles loaded with fisetin to improve anti-cancer therapy. Int J Biol Macromol 125:700–710
Fleming M, Ravula S, Tatishchev SF, Wang HL (2012) Colorectal carcinoma: pathologic aspects. J Gastrointest Oncol 3(3):153–173
Gupta R, Kadhim MM, Turki Jalil A, Obayes AM, Aminov Z, Alsaikhan F, Ramírez-Coronel AA, Ramaiah P, Tayyib NA, Luo X (2023) Multifaceted role of NF-κB in hepatocellular carcinoma therapy: molecular landscape, therapeutic compounds and nanomaterial approaches. Environ Res 228:115767
Hamilton SR, Aaltonen LA (2000) Carcinoma of the colon and rectum. Pathology and genetics of tumours of the digestive system, vol 2, 3rd edn. WHO classification of Tumours
Haque S, Morris JC (2017) Transforming growth factor-β: a therapeutic target for cancer. Hum Vaccin Immunother 13(8):1741–1750
Hassan HFH, Mansour AM, Salama SA, El-Sayed E-SM (2021) The chemopreventive effect of thymol against dimethylhydrazine and/or high fat diet-induced colon cancer in rats: relevance to NF-κB. Life Sci 274:119335
Hong SP (2014) Malignant Tumors in Colon. In Clinical Gastrointestinal Endoscopy: A Comprehensive Atlas: Springer, 475–498.
Ho WE, Peh HY, Chan TK, Wong WF (2014) Artemisinins: pharmacological actions beyond anti-malarial. Pharmacol Ther 142(1):126–139
Hu D, Wang Y, Chen Z, Ma Z, You Q, Zhang X, Zhou T, Xiao Y, Liang Q, Tan H, Xiao C (2014) Artemisinin protects against dextran sulfate-sodium-induced inflammatory bowel disease, which is associated with activation of the pregnane X receptor. Eur J Pharmacol 738:273–284
Huai M, Zeng J, Ge W (2021) Artemisinin ameliorates intestinal inflammation by skewing macrophages to the M2 phenotype and inhibiting epithelial–mesenchymal transition. Int Immunopharmacol 91:107284
Idikio HA (2011) Human cancer classification: a systems biology- based model integrating morphology, cancer stem cells, proteomics, and genomics. J Cancer 2:107
Jia Y, Xu G, Zhou W, Wang Z, Meng L, Zhou S, Xu X, Yuan H, Tian K (2014) Diabetes promotes DMH-induced colorectal cancer by increasing the activity of glycolytic enzymes in rats. PLoS ONE 9(10):e110455
Johansson ME, Hansson GC (2016) Immunological aspects of intestinal mucus and mucins. Nat Rev Immunol 16(10):639–649
Keshavarz MH, Ramadan A, Mousaviazar A, Zali A, Esmaeilpour K, Atabaki F, Shokrolahi A (2011) Reducing dangerous effects of unsymmetrical dimethylhydrazine as a liquid propellant by addition of hydroxyethylhydrazine Part I: physical properties. J Energ Mater 29(1):46–60
Khan R, Rehman MU, Khan AQ, Tahir M, Sultana S (2018) Glycyrrhizic acid suppresses 1, 2-dimethylhydrazine-induced colon tumorigenesis in Wistar rats: Alleviation of inflammatory, proliferation, angiogenic, and apoptotic markers. Environ Toxicol 33(12):1272–1283
Kim S, Jeong S (2019) Mutation hotspots in the β-catenin gene: lessons from the human cancer genome databases. Mol Cells 42(1):8–16
Klampfer L (2011) Cytokines, inflammation and colon cancer. Curr Cancer Drug Targets 11(4):451–464
Krishna S, Bustamante L, Haynes RK, Staines HM (2008) Artemisinins: their growing importance in medicine. Trends Pharmacol Sci 29(10):520–527

Krishna S, Ganapathi S, Ster IC, Saeed ME, Cowan M, Finlayson C, Kovacsevics H, Jansen H, Kremsner PG, Efferth T, Kumar D (2015) A randomised, double blind, placebo-controlled pilot study of oral artesunate therapy for colorectal cancer. EBioMedicine 2(1):82–90
Kumar S, Agnihotri N (2021) Piperlongumine targets NF-κB and its downstream signaling pathways to suppress tumor growth and metastatic potential in experimental colon cancer. Mol Cell Biochem 476(4):1765–1781
Kumar VL, Verma S, Das P (2019) Artesunate suppresses inflammation and oxidative stress in a rat model of colorectal cancer. Drug Dev Res 80(8):1089–1097
Lai H, Singh NP (2006) Oral artemisinin prevents and delays the development of 7, 12-dimethylbenz [a] anthracene (DMBA)-induced breast cancer in the rat. Cancer Lett 231(1):43–48
Lam NS, Long X, Su X-z, Lu F (2018) Artemisinin and its derivatives in treating helminthic infections beyond schistosomiasis. Pharmacol Res 133:77–100
Lan YT, Chang SC, Lin PC, Lin CC, Lin HH, Huang SC, Lin CH, Liang WY, Chen WS, Jiang JK, Lin JK, Yang SH (2021) Clinicopathological and molecular features of colorectal cancer patients with mucinous and non-mucinous adenocarcinoma. Front Oncol 11:620146
Li LN, Zhang HD, Yuan SJ, Tian ZY, Wang L, Sun ZX (2007) Artesunate attenuates the growth of human colorectal carcinoma and inhibits hyperactive Wnt/β-catenin pathway. Int J Cancer 121(6):1360–1635
Li LN, Zhang HD, Yuan SJ, Yang DX, Wang L, Sun ZX (2008) Differential sensitivity of colorectal cancer cell lines to artesunate is associated with expression of beta-catenin and E-cadherin. Eur J Pharmacol 588(1):1–8
Li N, Zhang S, Luo Q, Yuan F, Feng R, Chen X, Yang S (2019) The effect of dihydroartemisinin on the malignancy and epithelial-mesenchymal transition of gastric cancer cells. Curr Pharm Biotechnol 20(9):719–726
Li C, Zhao Z, Zhang J, Diao P, Li Y, Zhang Q, Zhang L (2020a) Effects of artemisinin on colon cancer cell proliferation through miR-22. J Biomater Tissue Eng 10(10):1447–1451
Li Y, Zhou X, Liu J, Gao N, Yang R, Wang Q, Ji J, Ma L, He Q (2020b) Dihydroartemisinin inhibits the tumorigenesis and metastasis of breast cancer via downregulating CIZ1 expression associated with TGF-β1 signaling. Life Sci 248:117454
Liang W, Liu J, Wu H, Qiao X, Lu X, Liu Y, Zhu H, Ma L (2019) Artemisinin induced reversal of EMT affects the molecular biological activity of ovarian cancer SKOV3 cell lines. Oncol Lett 18(3):3407–3414
Lin C, Yang L (2018) Long noncoding RNA in cancer: wiring signaling circuitry. Trends Cell Biol 28(4):287–301
Lin L, Lu W, Dai T, Chen H, Wang T, Yang L, Yang X, Liu Y, Sun D (2021) Novel artemisinin derivatives with potent anticancer activities and the anti-colorectal cancer effect by the mitochondria-mediated pathway. Bioorg Chem 106:104496
Maeda H, Nakamura H, Fang J, The EP (2013) Effect for macromolecular drug delivery to solid tumors: improvement of tumor uptake, lowering of systemic toxicity, and distinct tumor imaging in vivo. Adv Drug Deliv Rev 65(1):71–79
Malati T (2007) Tumour markers: an overview. Indian J Clin Biochem 22:17–31
Mariani F, Sena P, Roncucci L (2014) Inflammatory pathways in the early steps of colorectal cancer development. World J Gastroenterol 20(29):9716
Mármol I, Sánchez-de-Diego C, Pradilla Dieste A, Cerrada E, Rodriguez Yoldi MJ (2017) Colorectal carcinoma: a general overview and future perspectives in colorectal cancer. Int J Mol Sci 18(1):197
Mata R, Nakkala JR, Sadras SR (2023) Therapeutic role of biogenic silver and gold nanoparticles against a DMH-induced colon cancer model. Biomater Adv 146:213279
Mishra B, Patel BB, Tiwari S (2010) Colloidal nanocarriers: a review on formulation technology, types and applications toward targeted drug delivery. Nanomedicine 6(1):9–24
Mohamed SMS, Amin AM, Skander SW, Hewala TIM, Saleh EOM, Salih A (2022) Chemoprevention of 1, 2 dimethyl hydrazine-induced colon tumor in Albino rat by meloxicam and its correlation with immunoassay of serum CEA. Am J Biomed Sci 14(4):154–166
Mohammadzadeh P, Noroozi Gorgani B, Ghiasi S (2024) Alterations in P53 gene expression in experimental colon carcinoma of wistar rat. Turk J Oncol. https://doi.org/10.5505/tjo.2024.3774
Nagtegaal ID, Odze RD, Klimstra D, Paradis V, Rugge M, Schirmacher P, Washington KM, Carneiro F, Cree IA (2020) WHO Classification of Tumours Editorial Board. The 2019 WHO classification of tumours of the digestive system. Histopathology 76(2):182–188
Nakatani H, Kumon T, Kumon M, Hamada S, Okanoue T, Kawamura A, Nakatani K, Hiroi M, Hanazaki K (2012) High serum levels of both carcinoembryonic antigen and carbohydrate antigen 19–9 in a patient with sigmoid colon cancer without metastasis. J Med Invest 59(3.4):280–283
Nam W, Tak J, Ryu JK, Jung M, Yook JI, Kim HJ, Kim HJ, Cha IH (2007) Effects of artemisinin and its derivatives on growth inhibition and apoptosis of oral cancer cells. Head Neck J Sci Specialties Head Neck 29(4):335–340
Nguyen LH, Goel A, Chung DC (2020) Pathways of colorectal carcinogenesis. Gastroenterology 158(2):291–302
Nojadeh JN, Behrouz Sharif S, Sakhinia E (2018) Microsatellite instability in colorectal cancer. EXCLI J 17:159–168
Nusse R, Clevers H (2017) Wnt/β-catenin signaling, disease, and emerging therapeutic modalities. Cell 169(6):985–999
Pai RK, Jairath V, Casteele NV, Rieder F, Parker CE, Lauwers GY (2018) The emerging role of histologic disease activity assessment in ulcerative colitis. Gastrointest Endosc 88:887–898
Patel M, Horgan PG, McMillan DC, Edwards J (2018) NF-κB pathways in the development and progression of colorectal cancer. Transl Res 197:43–56
Patyar S, Patyar RR, Medhi B, Khanduja KL (2017) Chemopreventive effect of artesunate in 1, 2-dimethylhydrazine-induced rat colon carcinogenesis. J Adv Pharm Technol Res 8(3):102–107
Perše M, Cerar A (2005) The dimethylhydrazine induced colorectal tumours in rat-experimental colorectal carcinogenesis. Radiol Oncol 39(1):61–70
Rajendran MS, Jayaraman S, Khan JM, Jasmine S, Prabhakaran R, Raju MV, Chandrasekaran MK, Ahalliya RM, Kannappan P, Palanisamy CP, Kanniappan GV (2024) Investigating the colon toxicity and carcinogenic role of monosodium glutamate compared with dimethylhydrazine in male Wistar rats: exploring the link to childhood colon cancer risk. J King Saud Univ Sci 36(11):103507
Reis CP, Neufeld RJ, Ribeiro AJ, Veiga F (2006) Nanoencapsulation I. Methods for preparation of drug-loaded polymeric nanoparticles. Nanomedicine 2(1):8–21

Roy S, He R, Kapoor A, Forman M, Mazzone JR, Posner GH, Arav-Boger R (2015) Inhibition of human cytomegalovirus replication by artemisinins: effects mediated through cell cycle modulation. Antimicrob Agents Chemother 59(7):3870–3879
Sadik NA (2013) Chemopreventive efficacy of green tea drinking against 1, 2-dimethyl hydrazine-induced rat colon carcinogenesis. Cell Biochem Funct 31(3):196–207
Sadik NAH, Shaker OG (2013) Inhibitory effect of a standardized pomegranate fruit extract on Wnt signalling in 1, 2-dimethylhydrazine induced rat colon carcinogenesis. Dig Dis Sci 58(9):2507–2517
Saini MK, Vaiphei K, Sanyal SN (2012) Chemoprevention of DMH-induced rat colon carcinoma initiation by combination administration of piroxicam and C-phycocyanin. Mol Cell Biochem 361:217–228
Sakamoto K, Maeda S, Hikiba Y, Nakagawa H, Hayakawa Y, Shibata W, Yanai A, Ogura K, Omata M (2009) Constitutive NF-kappaB activation in colorectal carcinoma plays a key role in angiogenesis, promoting tumor growth. Clin Cancer Res 15(7):2248–2258
Sansom OJ, Meniel VS, Muncan V, Phesse TJ, Wilkins JA, Reed KR, Vass JK, Athineos D, Clevers H, Clarke AR (2007) Myc deletion rescues Apc deficiency in the small intestine. Nature 446(7136):676–679
Sayed A, Youssef EA, Mahmoud SA, Youssry S, Abdel-Mawla AA (2023) Effect of niclosamide on colorectal cancer induced by dimethylhydrazine in albino mice. Egypt J Basic Appl Sci 10(1):846–860
Schaefer KN, Peifer M (2019) Wnt/Beta-catenin signaling regulation and a role for biomolecular condensates. Dev Cell 48(4):429–444
Sharma SH, Thulasingam S, Nagarajan S (2017) Terpenoids as anti-colon cancer agents—a comprehensive review on its mechanistic perspectives. Eur J Pharmacol 795:169–178
Sharma SH, Kumar JS, Chellappan DR, Nagarajan S (2018) Molecular chemoprevention by morin—a plant flavonoid that targets nuclear factor kappa B in experimental colon cancer. Biomed Pharmacother 100:367–373
Shojaei-Zarghani S, Rafraf M, Khosroushahi AY, Sheikh-Najafi S (2020) Effectiveness of theobromine on inhibition of 1, 2-dimethylhydrazine-induced rat colon cancer by suppression of the Akt/GSK3β/β-catenin signaling pathway. J Funct Foods 75:104293
Shree A, Islam J, Vafa A, Mohammad Afzal S, Sultana S (2020) Gallic acid prevents 1, 2-dimethylhydrazine induced colon inflammation, toxicity, mucin depletion, and goblet cell disintegration. Environ Toxicol 35(6):652–664
Shree A, Islam J, Sultana S (2021) Quercetin ameliorates reactive oxygen species generation, inflammation, mucus depletion, goblet disintegration, and tumor multiplicity in colon cancer: probable role of adenomatous polyposis coli, β-catenin. Phytother Res 35(4):2171–2184
Shree A, Islam J, Yadav V, Sultana S, Khan HA (2022) Hesperetin alleviates DMH induced toxicity via suppressing oxidative stress and inflammation in the colon of Wistar rats. Environ Toxicol 37(9):2153–2166
Silva VR, Santos LS, Dias RB, Quadros CA, Bezerra DP (2021) Emerging agents that target signaling pathways to eradicate colorectal cancer stem cells. Cancer Commun (Lond) 41(12):1275–1313
Slaoui M, Fiette L (2011) Histopathology procedures: from tissue sampling to histopathological evaluation. Methods Mol Biol 691:69–82
Song J, Shu H, Zhang L, Xiong J (2019) Long noncoding RNA GAS5 inhibits angiogenesis and metastasis of colorectal cancer through the Wnt/β-catenin signaling pathway. J Cell Biochem 120(5):6937–6951
Sun G, Zhao S, Fan Z, Wang Y, Liu H, Cao H, Sun G, Huang T, Cai H, Pan H, Rong D (2023) CHSY1 promotes CD8+ T cell exhaustion through activation of succinate metabolism pathway leading to colorectal cancer liver metastasis based on CRISPR/Cas9 screening. J Exp Clin Cancer Res 42(1):248
Sung H, Ferlay J, Siegel RL, Laversanne M, Soerjomataram I, Jemal A, Bray F (2021) Global cancer statistics 2020: GLOBOCAN estimates of incidence and mortality worldwide for 36 cancers in 185 countries. CA Cancer J Clin 71(3):209–249
Talman AM, Clain J, Duval R, Ménard R, Ariey F (2019) Artemisinin bioactivity and resistance in malaria parasites. Trends Parasitol 35(12):953–963
Tanaka T (2009) Colorectal carcinogenesis: review of human and experimental animal studies. J Carcinog 8:5
Ten Berge D, Kurek D, Blauwkamp T, Koole W, Maas A, Eroglu E, Siu RK, Nusse R (2011) Embryonic stem cells require Wnt proteins to prevent differentiation to epiblast stem cells. Nat Cell Biol 13(9):1070–1075
Tong Y, Liu Y, Zheng H, Zheng L, Liu W, Wu J, Ou R, Zhang G, Li F, Hu M, Liu Z, Lu L (2016) Artemisinin and its derivatives can significantly inhibit lung tumorigenesis and tumor metastasis through Wnt/β-catenin signaling. Oncotarget 7(21):31413–31428
Tran BN, Nguyen HT, Kim JO, Yong CS, Nguyen CN (2017) Developing combination of artesunate with paclitaxel loaded into poly-d, l-lactic-co-glycolic acid nanoparticle for systemic delivery to exhibit synergic chemotherapeutic response. Drug Dev Ind Pharm 43(12):1952–1962
Vivanco I, Sawyers CL (2002) The phosphatidylinositol 3-Kinase AKT pathway in human cancer. Nat Rev Cancer 2(7):489–501
Voboril R, Weberova-Voborilova J (2006) Constitutive NF-kappaB activity in colorectal cancer cells impact on radiation-induced NF-kappaB activity, radiosensitivity, and apoptosis. Neoplasma 53(6):518–523
Vural S, Muhtaroğlu A, Uygur F (2023) The relationship between preoperative CEA and CA19-9 status and patient characteristics and lymph node involvement in early-stage colon cancer. Eur Rev Med Pharmacol Sci 27(10):4563–4569
Wang KS, Li J, Wang Z, Mi C, Ma J, Piao LX, Xu GH, Li X, Jin X (2017) Artemisinin inhibits inflammatory response via regulating NF-κB and MAPK signaling pathways. Immunopharmacol Immunotoxicol 39(1):28–36
Wang XZ, Zhang SF, Yang ZH, Ye ZW, Liu J (2020a) Punicalagin suppresses osteosarcoma growth and metastasis by regulating NF-κB signaling. J Biol Regul Homeost Agents 34(5):1699–1708
Wang Y, Chen Y, Liu L, He D, Li H (2020b) Effects of artemisinin combined with 5-fluorouracil on colon cancer cell proliferation, migration, and drug sensitivity via PI3K/AKT signaling. J Biomater Tissue Eng 10(11):1600–1604
Weifeng T, Feng S, Xiangji L, Changqing S, Zhiquan Q, Huazhong Z, Peining Y, Yong Y, Mengchao W, Xiaoqing J, Wan-Yee L (2011) Artemisinin inhibits in vitro and in vivo invasion and metastasis of human hepatocellular carcinoma cells. Phytomedicine 18(2–3):158–162

Wen L, Liu L, Wen L, Yu T, Wei F (2018) Artesunate promotes G2/M cell cycle arrest in MCF7 breast cancer cells through ATM activation. Breast Cancer 25:681–686
Wen L, Chan BCL, Qiu MH, Leung P-C, Wong CK (2024) Artemisinin and its derivatives as potential anticancer agents. Molecules 29(16):3886
Wu R, Gao Y, Wu J, Wang C, Yang L (2020) Semi-synthetic product dihydroartemisinin inhibited fibronectin-1 and integrin-β1 and interfered with the migration of HCCLM6 cells via PI3K-AKT pathway. Biotechnol Lett 42(6):917–926
Xi Y, Xu P (2021) Global colorectal cancer burden in 2020 and projections to 2040. Transl Oncol 14(10):101174
Xu X, Hu Y, Zhang LP, Liu B, Yang Y, Tang T, Tian J, Peng K, Liu T (2020) Lactic-co-glycolic acid-coated methylene blue nanoparticles with enhanced antibacterial activity for efficient wound healing. RSC Adv 10(21):12304–12307
Yallapu MM, Gupta BK, Jaggi M, Chauhan SC (2010) Fabrication of curcumin encapsulated PLGA nanoparticles for improved therapeutic effects in metastatic cancer cells. J Colloid Interface Sci 351(1):19–29
Yang W, Liu L, Li C, Luo N, Chen R, Li L, Yu F, Cheng Z (2018) TRIM52 plays an oncogenic role in ovarian cancer associated with NF-kB pathway. Cell Death Dis 9(9):908
Yao Y, Guo Q, Cao Y, Qiu Y, Tan R, Yu Z, Zhou Y, Lu N (2018) Artemisinin derivatives inactivate cancer-associated fibroblasts through suppressing TGF-β signaling in breast cancer. J Exp Clin Cancer Res 37(1):282
Yin S, Yang H, Tao Y, Wei S, Li L, Liu M, Li J (2020) Artesunate ameliorates DSS-induced ulcerative colitis by protecting intestinal barrier and inhibiting inflammatory response. Inflammation 43:765–776
Yu W, Liu C, Li X, Yang F, Cheng L, Liu C, Song Y (2017) Inositol hexaphosphate suppresses colorectal cancer cell proliferation via the Akt/GSK-3β/β-catenin signaling cascade in a 1, 2-dimethylhydrazine-induced rat model. Eur J Pharmacol 805:67–74
Zeng ZW, Chen D, Chen L, He B, Li YA (2023) comprehensive overview of Artemisinin and its derivatives as anticancer agents. Eur J Med Chem 247:115000
Zhang Y, Wang X (2020) Targeting the Wnt/β-catenin signaling pathway in cancer. J Hematol Oncol 13(1):165
Zhang Y, Xu G, Zhang S, Wang D, Saravana Prabha P, Zuo Z (2018) Antitumor research on artemisinin and its bioactive derivatives. Nat Prod Bioprospect 8(4):303–319
Zhang B, Liu P, Zhou Y, Chen Z, He Y, Mo M, Dai G, Xia W, Du Y, Liu Y, Chen X (2019) Dihydroartemisinin attenuates renal fibrosis through regulation of fibroblast proliferation and differentiation. Life Sci 223:29–37
Zhao X, Ma L, Dai L, Zuo D, Li X, Zhu H, Xu F (2020) TNF-α promotes the malignant transformation of intestinal stem cells through the NF-κB and Wnt/β-catenin signaling pathways. Oncol Rep 44(2):577–588
Zheng L, Pan J (2018) The anti-malarial drug artesunate blocks Wnt/β-catenin pathway and inhibits growth, migration and invasion of uveal melanoma cells. Curr Cancer Drug Targets 18(10):988–998
Zhou ZH, Chen FX, Xu WR, Qian H, Sun LQ, Lü XT, Chen L, Zhang J, Ji HC, Fei SJ (2013) Enhancement effect of dihydroartemisinin on human γδ T cell proliferation and killing pancreatic cancer cells. Int Immunopharmacol 17(3):850–857
Zhou Y, Wang X, Zhang J, He A, Wang YL, Han K, Su Y, Yin J, Lv X, Hu H (2017) Artesunate suppresses the viability and mobility of prostate cancer cells through UCA1, the sponge of miR-184. Oncotarget 8(11):18260
Zhou Y, Li X, Chen K, Ba Q, Zhang X, Li J, Wang J, Wang H, Liu H (2021) Structural optimization and biological evaluation for novel artemisinin derivatives against liver and ovarian cancers. Eur J Med Chem 211:113000
Zhu QC, Gao RY, Wu W, Guo BM, Peng JY, Qin HL (2014) Effect of a high-fat diet in development of colonic adenoma in an animal model. World J Gastroenterol 20(25):8119

Publisher's Note